Maury Martins de Oliveira Júnior

Thermodynamic and Cost Analysis of the Organic Rankine Energy Storage (ORES) system

Belo Horizonte, Brasil

Julho, 2020

Maury Martins de Oliveira Júnior

Thermodynamic and Cost Analysis of the Organic Rankine Energy Storage (ORES) system

Tese apresentada ao Programa de Pós-graduação em Engenharia Mecânica da Universidade Federal de Minas Gerais como requisito parcial à obtenção do título de Doutor em Engenharia Mecânica.

Universidade Federal de Minas Gerais

Escola de Engenharia

Programa de Pós-Graduação em Engenharia Mecânica

Orientador: Prof. Matheus Pereira Porto

Coorientador: Prof. Antônio Augusto Torres Maia

Belo Horizonte, Brasil

Julho, 2020

Oliveira Júnior, Maury Martins de.
O48t Thermodynamic and cost analysis of Organic Rankine Energy Storage (ORES) systems [recurso eletrônico] / Maury Martins de Oliveira Júnior. - 2020.
1 recurso online (81 f. : il., color.) : pdf.

Orientador: Matheus Pereira Porto.
Coorientador: Antônio Augusto Torres Maia.

Tese (doutorado) - Universidade Federal de Minas Gerais, Escola de Engenharia.

Bibliografia: f. 73-81.
Exigências do sistema: Adobe Acrobat Reader.

1. Engenharia mecânica - Teses. 2. Energia - Armazenamento - Teses. 3. Fluidos - Teses. I. Porto, Matheus Pereira. II. Maia, Antônio Augusto Torres. III. Universidade Federal de Minas Gerais. Escola de Engenharia. IV. Título.

CDU: 621(043)

Ficha catalográfica: Biblioteca Profº Mário Werneck, Escola de Engenharia da UFMG

UNIVERSIDADE FEDERAL DE MINAS GERAIS
ESCOLA DE ENGENHARIA
PROGRAMA DE PÓS-GRADUAÇÃO EM ENGENHARIA MECÂNICA

FOLHA DE APROVAÇÃO

THERMODYNAMIC AND COST ANALYSIS OF ORGANIC RANKINE ENERGY STORAGE (ORES) SYSTEMS

MAURY MARTINS DE OLIVEIRA JÚNIOR

Tese submetida à Banca Examinadora designada pelo Colegiado do Programa de Pós-Graduação em Engenharia Mecânica da Universidade Federal de Minas Gerais, constituída pelos Professores: Dr. Matheus Pereira Porto (orientador/Departamento de Engenharia Mecânica/UFMG), Dr. Antonio Augusto Torres Maia (coorientador/Departamento de Engenharia Mecânica/UFMG), Dr. Thales Alexandre Carvalho Maia (Departamento de Engenharia Elétrica/UFMG), Jonathan Radcliffe (Universityof Birmingham), Paulo Alexandre Costa Rocha (Universidade Federal do Ceará) e Rafael Augusto Magalhães Ferreira (Departamento de Engenharia Mecânica/UFMG), como parte dos requisitos necessários à obtenção do título de **"Doutor em Engenharia Mecânica"**, na área de concentração de **"Energia e Sustentabilidade".**

Tese aprovada no dia 03 de agosto de 2020.

Por:

Documento assinado eletronicamente por **Antonio Augusto Torres Maia**, **Professor do Magistério Superior**, em 25/09/2020, às 08:01, conforme horário oficial de Brasília, com fundamento no art. 6º, § 1º, do Decreto nº 8.539, de 8 de outubro de 2015.

Documento assinado eletronicamente por **Rafael Augusto Magalhães Ferreira**, **Professor do Magistério Superior**, em 27/09/2020, às 21:43, conforme horário oficial de Brasília, com fundamento no art. 6º, § 1º, do Decreto nº 8.539, de 8 de outubro de 2015.

Documento assinado eletronicamente por **Paulo Alexandre Costa Rocha**, **Usuário Externo**, em 27/09/2020, às 22:44, conforme horário oficial de Brasília, com fundamento no art. 6º, § 1º, do Decreto nº 8.539, de 8 de outubro de 2015.

Documento assinado eletronicamente por **Thales Alexandre Carvalho Maia**, **Professor do Magistério Superior**, em 28/09/2020, às 11:52, conforme horário oficial de Brasília, com fundamento no art. 6º, § 1º, do Decreto nº 8.539, de 8 de outubro de 2015.

Documento assinado eletronicamente por **Jonathan Radcliffe**, **Usuário Externo**, em 05/10/2020, às 13:53, conforme horário oficial de Brasília, com fundamento no art. 6º, § 1º, do Decreto nº 8.539, de 8 de outubro de 2015.

Documento assinado eletronicamente por **Matheus Pereira Porto**, **Servidor(a)**, em 07/10/2020, às 07:43, conforme horário oficial de Brasília, com fundamento no art. 6º, § 1º, do Decreto nº 8.539, de 8 de outubro de 2015.

Agradecimentos

Gostaria de, primeiramente, agradecer à CAPES e ao CNPq pelo apoio financeiro prestado ao longo do desenvolvimento deste trabalho, sem o qual a minha formação e este trabalho não teriam sido concluídos.

Também gostaria de agradecer à dedicação do meu orientador, Prof. Matheus Pereira Porto, que desde 2015 se dispôs a me acompanhar nesta empreitada, e do meu coorientador, Prof. Antônio Augusto Torres Maia, pela disposição, paciência e sabedoria desde a época em que trabalhei em seu laboratório durante a graduação. Gostaria de agradecer ao DEMEC e seus membros, em especial à Marina, ao Edison e ao Lázaro, pela assistência com questões práticas assim como técnicas. Aos colegas de laboratório/DEMEC (Leonardo, Ramon, Daniel, Rafael, Alessandro, Kelvin, Luciano, Gabriel, Bruno Todde, Bruno Phillip, João Vitor, Osvaldo, Tomás, Vitor, Hebert, Clara, Vanessa) que contribuíram com a minha formação das mais diversas maneiras, desde esclarecendo conceitos ou sugestões aos momentos lúdicos e descontraídos.

I would also like to thank my advisors at the University of Birmingham, Prof. Yulong Ding and, especially, Prof. Jonathan Radcliffe, just as other members of the UoB that helped me make the most of my time at Birmingham, namely Adriano, Sue, Coral, Niko, Konstantina, Ellen, Natacha, Coco, Helena, Alex, Sharon, Jon and the Navs members, Ma and Dal.

Aos meus amigos da época da graduação, do mestrado e aos defensores da torre que continuaram me apoiando ao longo do meu doutorado. Agradecer à minha família, em especial meus padrinhos Tio Ronaldo e Tia Marília, avó Aracy, ao Tio Kléber e Tia Mônica pelos ensinamentos e carinho, meus pais e meu irmão. Também gostaria de agradecer à minha esposa Daniela por todo o apoio, carinho e paciência.

"The scientific man does not aim at an immediate result. He does not expect that his advanced ideas will be readily taken up. His work is like that of the planter — for the future. His duty is to lay the foundation for those who are to come, and point the way. He lives and labors and hopes."

Nikola Tesla

Abstract

CAES (Compressed Air Energy Storage) and LAES (Liquid Air Energy Storage) are two of the most promising long-term energy storage solutions. However, CAES requires robust equipments and components due to the higher working pressures involved and also lower energy density, while LAES requires air liquefaction cycles, which imposes a relevant restriction to efficiency and increase costs. This work evaluated the potential use of organic fluids as an energy storage medium and proposed an energy storage system, named ORES (Organic Rankine Energy Storage) as an alternative to LAES and CAES. The objective of the ORES system is to gather some of the qualities and mitigate some of the drawbacks of both CAES and LAES. This study first focused on the evaluation of the potential of organic fluids as an energy storage medium in terms of exergy density and cost of the storage system (tank and fluid). Before evaluating the storage system, a set of five organic fluids was selected based on technical maturity, safety and environmental factors, namely R-152a, R-134a, R-142b, R-365mfc and R-141b. The evaluation of the potential of organic fluids as an energy storage medium showed that all of the evaluated working fluids achieved an exergy density higher than that of compressed air. The maximum exergy density for the organic fluids ranged from 8 to 15 kWh m^{-3} for pressures up to 4,200 kPa while the maximum exergy density for compressed air is 6.5 kWh m^{-3} and 180 kWh m^{-3} for liquid air. The cost of the storage system (tank and fluid) was found to be around 33% cheaper for the organic fluids close to their respective critical pressure when compared to the cost for compressed air at common CAES operational pressure (8,000 kPa). Then, the cost per unit exergy was calculated, R-152a, R-134a and R-142b had the lower cost per unit exergy. While the minimum cost per unit exergy for compressed air ranged from 3,000 to 5,000 \$ kWh^{-1}, the cost for R-152a, R-134a and R-142b ranged from 1,000 to 2,000 \$ kWh^{-1} for storage volumes of 2 and 10 m^3, respectively. In the second part of this study, a novel energy storage system based on the ORC (Organic Rankine Cycle) was proposed. The ORES system was evaluated under a quasi-steady state analysis and transient analysis for the same fluids as for the organic fluid potential analysis. The quasi-steady state analysis evaluated the effects of pressure at the HPT (High Pressure Tank) and the superheating degree on round-trip efficiency and the transient analysis evaluated the effects of high and low pressure tank volume on efficiency, energy density and CAPEX. The round-trip efficiency of the ORES system was relatively high for both the quasi-steady state and transient analysis, reaching up to 74% and 73%, respectively, similar to that of CAES and LAES. However, the energy density for all organic fluids was lower than that of CAES, reaching only up to 2.29 kWh m^{-3} for R-365mfc. This study showed that organic fluids have the potential to be an alternative to CAES and LAES for medium-scale, long-duration, energy storage systems, both in terms of efficiency and cost. It is believed that the proposed system can be further improved and, potentially, surpass the energy density of CAES while also reducing CAPEX, which was already cheaper than CAES.

Keywords: Organic Rankine Cycle, intermittent energy generation, energy storage, organic fluid.

Resumo

Este trabalho avaliou o potencial uso de fluidos orgânicos como meio de armazenamento de energia e propõe um sistema de armazenamento de energia, chamado de Armazenamento de Energia Rankine Orgânico (ORES) como alternativa aos sistemas LAES (Armazenamento de Energia por Ar Liquido) e CAES (Armazenamento de Energia por Ar Comprimido). CAES e LAES são duas das principais alternativas para armazenamento de energia de longo prazo. No entanto, CAES requer equipamentos e componentes robustos para lidar com as elevadas pressões e também apresenta baixa densidade de energia, enquanto o LAES requer ciclos de liquefação de ar, o que impõe sérias restrições à eficiência e maior custo. O objetivo do sistema ORES é incorporar algumas das vantagens enquanto mitiga as desvantagens de ambos os sistemas CAES e LAES. Este estudo focou, inicialmente, na avaliação do potencial dos fluidos orgânicos como meios de armazenamento de energia em termos de densidade de exergia e do custo do sistema de armazenamento (tanque e fluido). Antes de avaliar o sistema de armazenamento, um conjunto de cinco fluidos orgânicos foram selecionados com base na maturidade técnica, segurança e fatores ambientais, R-152a, R-134a, R-142b, R-365mfc e R-141b. A avaliação do potencial de fluidos orgânicos como meio de armazenamento de energia mostrou que todos os fluidos avaliados atingiram densidade de exergia superior à do ar comprimido. A máxima densidade de exergia para os fluidos orgânicos variou de 8 a 15 kWh m^{-3} para pressões de até 4,200 kPa enquanto a máxima densidade de exergia para o ar comprimido é 6,5 kWh m^{-3} e para o ar líquido 180 kWh m^{-3}. O custo do sistema de armazenamento (tanque e fluido) para os fluidos orgânicos foi cerca de 33% menor quando comparados ao ar comprimido em condições operacionais comuns de sistemas CAES (8.000 kPa). O custo por unidade de exergia foi, então, calculado, sendo obtidos os menores valores para R-152a, R-134a e R-142b. Enquanto o custo por unidade de exergia mínimo para o ar comprimido variaram de 3.000 a 5.000 \$ kWh^{-1}, o custo para R-152a, R-134a e R-142b variou de 1.000 a 2.000 \$ kWh^{-1} para volumes de armazenamento de 2 e 10 m^3, respectivamente. Na segunda parte deste estudo um novo sistema de armazenamento de energia baseado do ORC (Ciclo Rankine Orgânico) é proposto. O sistema ORES proposto foi avaliado considerando uma análise em regime quase-permanente e uma análise transiente para os mesmos fluidos avaliados na análise do potencial dos fluidos orgânicos. A análise quase-permanente foi usada para avaliar os efeitos da pressão no HPT (tanque de alta pressão) e o grau de superaquecimento na eficiência de ciclo e a análise transiente foi usada para avaliar os efeitos do volume dos tanques de alta e baixa pressão, na eficiência, densidade energia e CAPEX do sistema. A eficiência de ciclo do sistema ORES obtida foi relativamente alta sob ambas a análise quasi-permanente e transiente, alcançando 74% e 73%, respectivamente, valores similares aos alcançados pelos sistemas CAES e LAES. No entanto, a densidade de energia do sistema ORES foi inferior ao do CAES, alcançando 2,29 kWh m^{-3} para o R-365mfc. Este estudo demonstrou que os fluidos orgânicos têm o potencial de se apresentar como alternativa aos sistemas CAES e LAES para armazenamento de energia em média escala e longa duração ambos em termos de eficiência e custo. Acredita-se que o sistema proposto pode ser aprimorado e, potencialmente, superar a densidade de energia do sistema CAES e ter seu CAPEX reduzido.

Palavras-chave: Ciclo Rankine Orgânico, Geração intermitente de energia, Armazenamento de Energia, Fluido orgânico.

List of Figures

List of Tables

List of abbreviations and acronyms

$CAPEX$	Capital expenditure
$CAES$	Compressed Air Energy Storage
$CCES$	Compressed CO_2 Energy Storage
$CEPCI$	Chemical Engineering Plant Cost Index
ESS	Energy Storage Systems
GWP	Global Warming Potential
HPT	High Pressure Storage Tank
LPT	Low Pressure Storage Tank
$LAES$	Liquid Air Energy Storage
ODP	Ozone Depletion Potential
ORC	Organic Rankine Cycle
$ORES$	Organic Rankine Energy Storage
$PHES$	Pumped Hydroelectric Energy Storage
$PTES$	Pumped Thermal Energy Storage
PV	Photovoltaic
SRC	Steam Rankine Cycle
TES	Thermal Energy Storage

List of symbols

C	Cost, USD
CA	Corrosion allowance, m
COP	Coefficient of performance
D_i	Storage tank internal diameter, m
E	Welded joint efficiency
F_M	Bare module material factor
F_P	Bare module pressure factor
h	Specific enthalpy, kJ kg^{-1}
I	Cost index
K	Volume multiplication factor
MDV	Minimum Design Volume, m^3
m	Mass in the tank, kg
$\dot{m}$	Mass flow rate, kg s^{-1}
P	Pressure, kPa
Q	Heat, kJ
q	Heat per unit mass, kJ kg^{-1}
S	Maximum allowable tension, kPa
s	Specific entropy, kJ kg^{-1} K^{-1}
T	Temperature, K
t	Time, s
t_{min}	Minimum tank thickness, m
U	Total internal energy, kJ
u	Specific internal energy, kJ kg^{-1}

V	Storage tank volume, m^3
v	Specific volume, m^3 kg^{-1}
W	Work, kJ
$\dot{W}$	Power, kW
w	Work per unit mass, kJ kg^{-1}
	Greek letters
χ	Specific exergy, kJ m^{-3}
ΔT_{SH}	Superheating at the turbine inlet, K
Δt	Process duration, s
η	Efficiency
ρ	Density, kg m^{-3}
	Subscripts
amb	Relative to ambient conditions
$barg$	Gauge pressure, bar
C	Relative to the condenser
Ch	Relative to the charging process
D	Relative to the discharging process
E_V	Energy density in terms of volume, kWh m^{-3}
E_m	Energy density in terms of mass, kWh kg^{-1}
$crit$	Relative to the critical state
Ev	Relative to the evaporator
fl	Relative to the working fluid
H	Relative to the heater
$HP1$	Relative to the heat pump of the discharging process
$HP2$	Relative to the heat pump of the charging process
HPT	Relative to the high pressure tank

L	Relative to the low temperature side of the heat pump
LPT	Relative to the low pressure tank
l	Saturated liquid state
o	Relative to the dead state
p	Relative to the pump
RT	Round-trip
st	Relative to the storage tank
s	Isentropic process
t	Relative to the turbine
χ, m	Exergy density in terms of mass, kJ kg^{-1}
χ, V	Exergy density in terms of volume, kJ m^{-3}

Contents

1 Introduction

Renewable energy systems, especially wind and solar energy, have increased rapidly in the past decades, surpassing 25% of the global electricity generation and are expected to reach up to 85% of total energy generation by 2050 (20). The intermittent nature of these systems poses a challenge to energy safety in scenarios of high renewable energy penetration as these can be highly variable. The reliability of energy supply in such scenarios can be increased by demand-side management, supply-side management, grid extension, energy storage systems and others. Amongst these solutions, energy storage systems are considered one of the most promising (21, 22, 23).

CAES (Compressed Air Energy Storage) represents the second largest bulk-scale energy storage system worldwide, in installed capacity (24, 25). Despite its low self-discharging rate, high energy storage capacity and long lifetime, CAES systems have a low energy density, therefore they require a large storage vessel, which may only be feasible when suitable geological formations are available. This restricts the application potential of CAES, likely resulting in increased costs and energy loss because of the longer distances of electric power transmission (26, 27).

LAES (Liquid Air Energy Storage) systems have been proposed as an alternative to CAES providing high energy storage capacity and low self-discharge rates without the geographical constraint, but at the expense of new challenges, mainly related to the air liquefaction process, which involves expensive equipment and has relatively low efficiency. In a LAES system the air is liquefied before storage, achieving a higher density, which makes it possible to store the air in artificial tanks, even for large scale systems (28, 29).

Recently some studies have proposed new alternatives in an attempt to avoid the main disadvantages of both CAES and LAES systems. Hybrid CAES-LAES system have been proposed, initially by (30) and afterwards by (31), with the objective of increasing energy density with the LAES tank whilst reducing the efficiency limitations of LAES and mitigating depressurization during discharge and the dependence on geological formations of CAES. New systems have also been proposed, such as the CCES (Compressed CO_2 Energy Storage) and PTES (Pumped Thermal energy storage) but are still on the earlier stages of development (5, 8, 32).

In contrast to air, many organic fluids can be stored at high pressures and ambient temperature in a liquid state, increasing energy density whilst still retaining the capacity to recover power. Organic fluids have replaced water as a working fluid in different engineering applications, generating power from low temperature heat sources and improving system efficiency (33, 34, 35, 36, 37). The ORC (Organic Rankine Cycle) is

one of the most studied cycles for organic fluids, usually with low or medium temperature heat sources, such as waste heat (34, 38, 39, 40), biomass (41, 42), solar thermal (33, 35) and geothermal (43, 44) power plants. ORC design can be highly flexible and complex as there are several organic fluids to choose from, each resulting in different optimal ORC parameters (19).

1.1 Objectives

The main objective of this study is to evaluate an alternative type of energy storage system, that uses organic working fluids instead of air as a working fluid. It is intended to achieve an energy density higher than that for CAES but with lower investment relative to LAES systems. The characteristics of the ORC indicate that this new energy storage system can be suitable for long-term, small to medium-scale applications, such as energy arbitrage, peak shaving and load leveling (25). This objective was divided in two parts. First, the potential of organic fluids as an energy storage medium was evaluated in terms of exergy density and of the storage system cost. In the second part, an energy storage system was proposed and evaluated, first in terms of efficiency based on a quasi-steady state analysis and then under a transient analysis in terms of round-trip efficiency, energy density and capital cost. All models developed in this study were implemented in MATLAB with the CoolProp library for thermodynamic properties (17).

1.2 Thesis structure

After this brief introduction, chapter two reviews energy storage systems, covering technologies, applications and markets. Chapter three covers the use of organic fluids in energy generation, including fluid selection, ORC optimization, main applications and design process. Chapter four presents a preliminary analysis of organic fluids as energy storage medium and chapter five presents a thermodynamic and cost analysis of the ORES (Organic Rankine Energy Storage). The final chapter presents the main conclusions and implications of the results obtained during this research along with suggestions of future studies based on this research.

2 Energy storage

Electric energy storage is one of the alternatives, other than transmission and distribution grids, demand and supply-side-management, to provide stability for power systems (45). The reliability of an energy system refers to its capacity to cope with fluctuations in supply and demand over different time scales, such as sudden energy outages, generator failure, or demand spikes (46). Energy storage systems have been used for several years to contribute to the reliability of an electric grid and have been increasingly needed due to the fast expansion of intermittent renewable energy sources, most notably solar and wind energy, which are responsible for increasing grid energy instability. A review work on research from 17 energy storage expansion studies involving over 400 scenarios of intermittent renewable energy in Europe and in the U.S. has concluded that as the renewable energy share increases, the energy storage power demand increases linearly, whilst the energy capacity demand increases exponentially. Therefore, significant energy storage capacity is needed for scenarios with over 25% share of renewable energy sources, a scenario that is becoming increasingly realistic all around the globe (45, 47).

This chapter will first present a brief introduction to energy markets, followed by an introduction to the main functions of energy storage in power systems, the different classifications of ESS (Energy Storage Systems), a description of the main performance indexes and, finally, a brief description of key long-term energy storage systems.

2.1 Energy management

The main task that must be pursued by electric grid operators is to balance the energy demand and supply in different time scales (seasonal, weekly, daily, hourly and transient). The total energy demand is composed of three main types of consumers: residential, commercial and industrial, each of these groups with a different consumption pattern (48). Seasonal variations are differences in consumption due to climate conditions, e.g. use of air conditioners and heaters. Weekly variations are related to the different consumption profiles during weekdays and the weekend (when residential consumption is higher while industrial and commercial demands are lower). Daily and Hourly variations occurs mostly due to residential consumption (as commercial and industrial are usually relatively stable) and related to consumption habits, e.g. higher demand during the period when people are returning home, preparing meals, using the shower, etc. And, finally, transient events are the result of random individual events (49). Figure 2.1 presents the Brazilian hourly load for June, 20th and December, 21st, both Fridays, and the Sundays June, 22nd and December 23rd, all for 2019, illustrating the difference between weekday

and weekend loads, summer and winter loads and hourly variations.

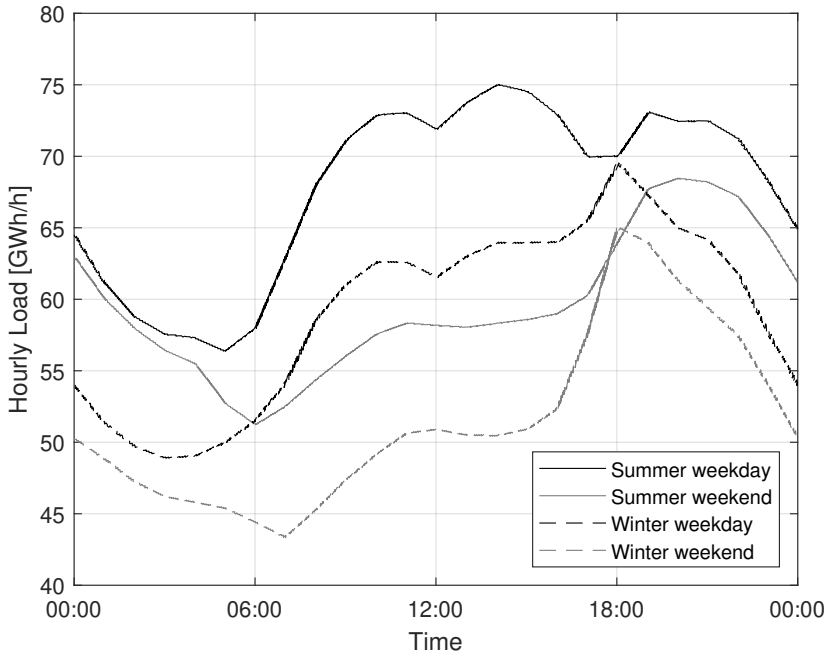

Figure 2.1 – Hourly Brazilian load for weekdays and weekends during winter and summer of 2019 (1).

In order to ensure a stable, reliable, constant supply of energy the electricity operator must anticipate and react to changes in the demand by activating the most suitable services to mitigate an excess or insufficient supply whilst minimizing energy cost, which is where ESS have their role (45).

2.2 Energy storage classifications

ESS are usually classified based either on the application of the system or on the form of the stored energy (21). ESS can be classified in three main groups based on their application: power quality, bridging power or energy management. Each of these groups are comprised of several services with a wide variety of requirements, constraints and economic opportunities (49, 50).

Energy management consists in bulk-storage of scales above 100 MW with hourly to daily output duration and storage for up to 4 months (50, 51, 52). Energy arbitrage is one of the main examples of this type of service, energy is bought from the grid during off-peak times, when energy price is low, and is sold to the grid during peak hours, when energy price is high.

Bridging power is characterized by energy supply over a period of seconds to minutes with the purpose of ensuring power continuity, usually applied when switching between two different power sources. ESS for power bridging are usually characterized by

moderate power (100 kW - 10 MW) and response time (around 1 s). For example, the operator can have a reasonable forecast for the increase in demand at the early hours of the day, therefore it schedules the operation of assets to follow the load curve during this period (49, 51).

Power quality applications require energy supply for short periods of time, a few seconds, and rapid cycling energy needs, sometimes caused by instabilities in energy generation or sudden peaks in energy demand, with the objective of assuring the continuous generation of power with the desired operational frequency and voltage. ESS for power quality must have low response time (order of milliseconds) to respond to sudden mismatches between supply and demand. One of the main services for power quality is frequency response services, e.g. frequency response services in the UK national grid are required to have a response time from 2 to 30 s and generation for up to 30 min, depending on the type of frequency response service (2). Figure 2.2 shows the frequency in the Great Britain electric grid with a 1 s resolution for a 30 min period and the operational limits of the system. In the Great Britain electric grid the frequency must be kept between 49.5 and 50.5 Hz, but a narrower interval is set by the operational limits in order to achieve a safety margin. In this scenario fast response services, such as Li-ion batteries, supercapacitors and FESS (Flywheel Energy Storage Systems), are connected to the grid and respond to changes in the grid frequency either continuously or when a determined frequency limit is crossed, depending on the contract with the grid operator (2).

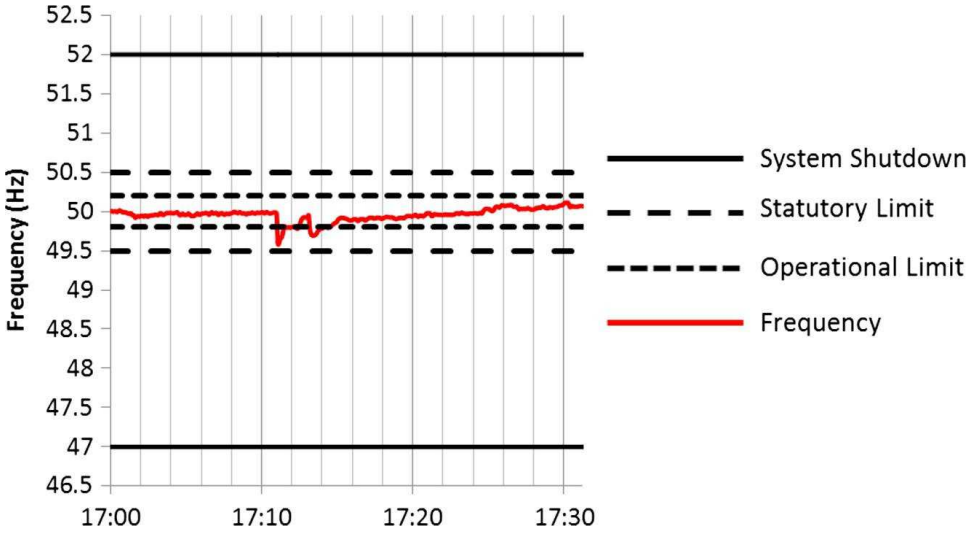

Figure 2.2 – Frequency variation in Great Britain and limits for operation (2).

The operation of a PV (Photovoltaic) system combined with a NaS battery is now presented to illustrate more clearly some of the applications of ESS in Figure 2.3. The system in Figure 2.3 is required to provide a constant power of 500 kW between 09:00 and 18:00 for this specific day. Without the ESS the PV system would only be able to provide the required power until 15:00, after this time it would need a complementary source to provide partly or completely the energy demand. The battery is then used to

relocate the surplus energy during high energy generation periods to later hours (Energy management) and also stabilise energy generation (Power quality). In the present case there is a period of energy shortage at around 12:00 h which uses the ESS to maintain energy supply at the required power output. It is important to note that the provided data is characteristic of a relatively clear day, during a cloudy or rainy day energy generation is more unstable and the impact of the ESS would be even more relevant (3). It should also be noted that this example also illustrates that an ESS can provide multiple services in the same installation.

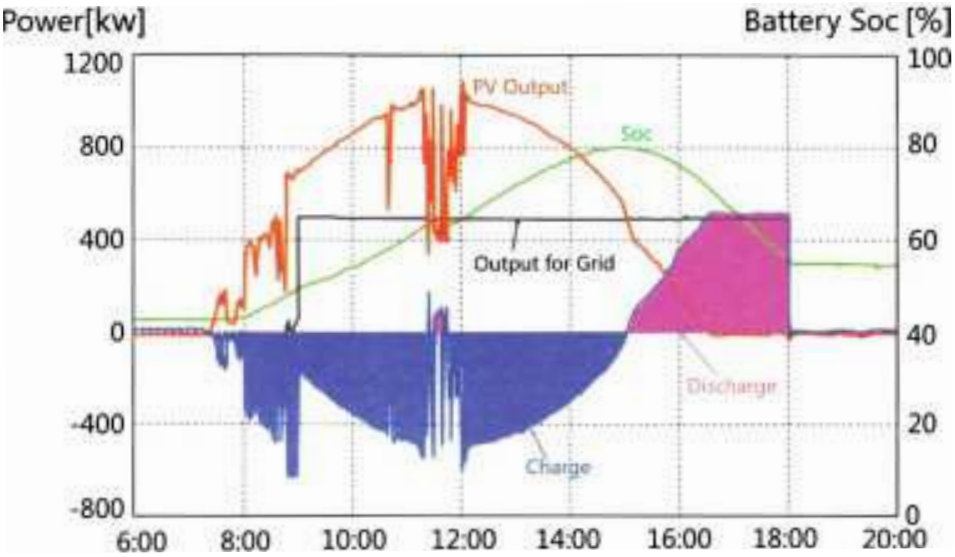

Figure 2.3 – Power and Battery State of Charge (SoC) over a day for a photovoltaic system combined with a NaS battery system (3).

Energy storage systems can also be classified based on the form of the stored energy, which is a more straightforward and intuitive approach. The classification for the main energy storage technologies is presented in Figure 2.4.

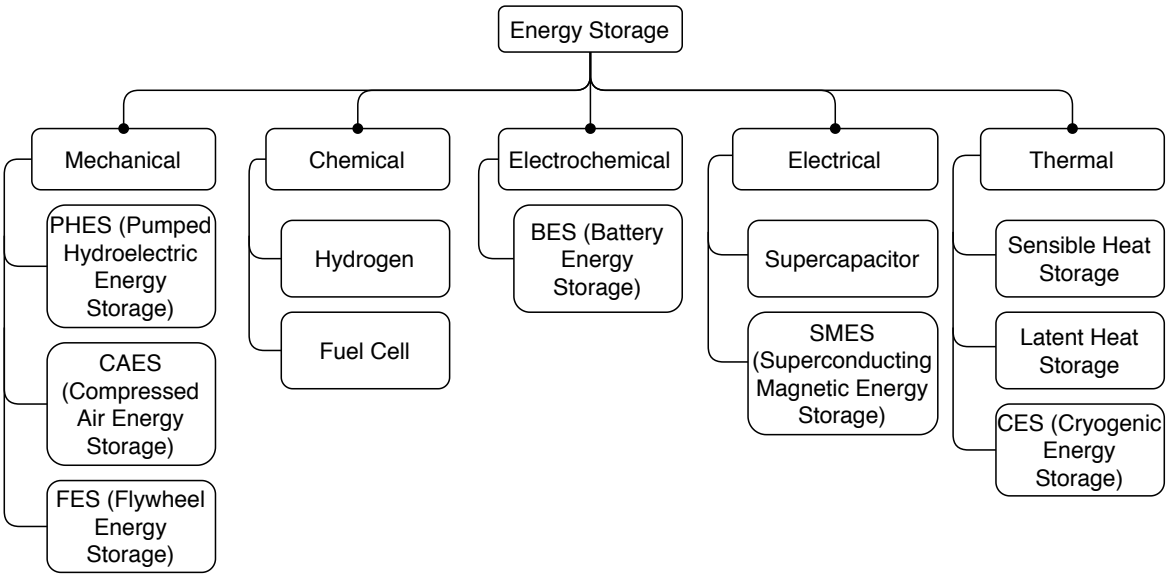

Figure 2.4 – Energy storage classification based on the form of stored energy.

2.3 Key performance indexes

In this section, the main performance indexes for the comparison of ESS are presented. Common indicators such as system life time, technological maturity, capital and operational costs should naturally be considered when evaluating potential ESS. The suitability of an ESS to each application group is linked to ESS characteristic parameters, such as power rating, response time, energy storage capacity and discharge duration. For example, CAES systems are capable of storing massive amounts of energy over a reasonable period of time (for days or even months) but are usually characterized by relatively high response times. Therefore, they are more indicated to bulk energy storage, whereas supercapacitors can provide considerable power almost instantaneously, but only for a short period of time, being indicated for intra-minute, power quality applications.

Round-trip efficiency, self-discharge rate, energy and power density are key parameters for the evaluation of ESS. The round-trip efficiency is defined as the ratio of net electric energy generated during discharge and the electric energy consumed during the charging process, representing an overall efficiency of the system. Most commercially mature ESS usually present an efficiency over 60 % (21). The self-discharge rate is the result of loss of energy during storage which can be dissipated in several forms and is a key factor in determining the ESS potential storage duration. For example, CAES have a low self-discharge rate due to air leakage and can store energy for months while supercapacitors have a high daily self-discharging rates which can range from 10 to 100 %, meaning they can lose all of their stored energy in a period of hours (21). The energy density is defined as the ratio between generated energy and the total mass or volume of the system. Depending on the type of energy density to be calculated, the energy density is particularly important as it indicates the required volume of the storage vessel, which

is directly related to storage capital cost and might also characterize a project constraint. The power density is similar to energy density but with the rated power on the nominator rather than the total generated energy (53). Figure 2.5a shows the range of parameters required by different applications and Fig. 2.5b shows the parameters of some of the main ESS. Power quality services, for example, require low to medium power ratings with a discharge time from minutes to hours, which can be provided by supercapacitors and flywheels, as illustrated in Fig. 2.5b.

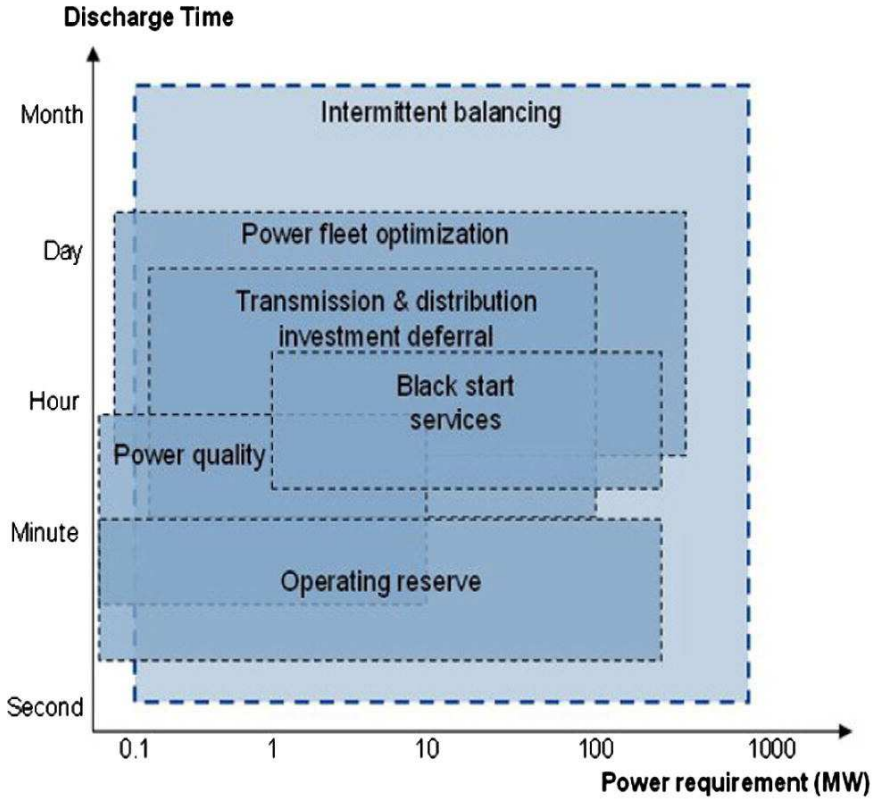

(a)

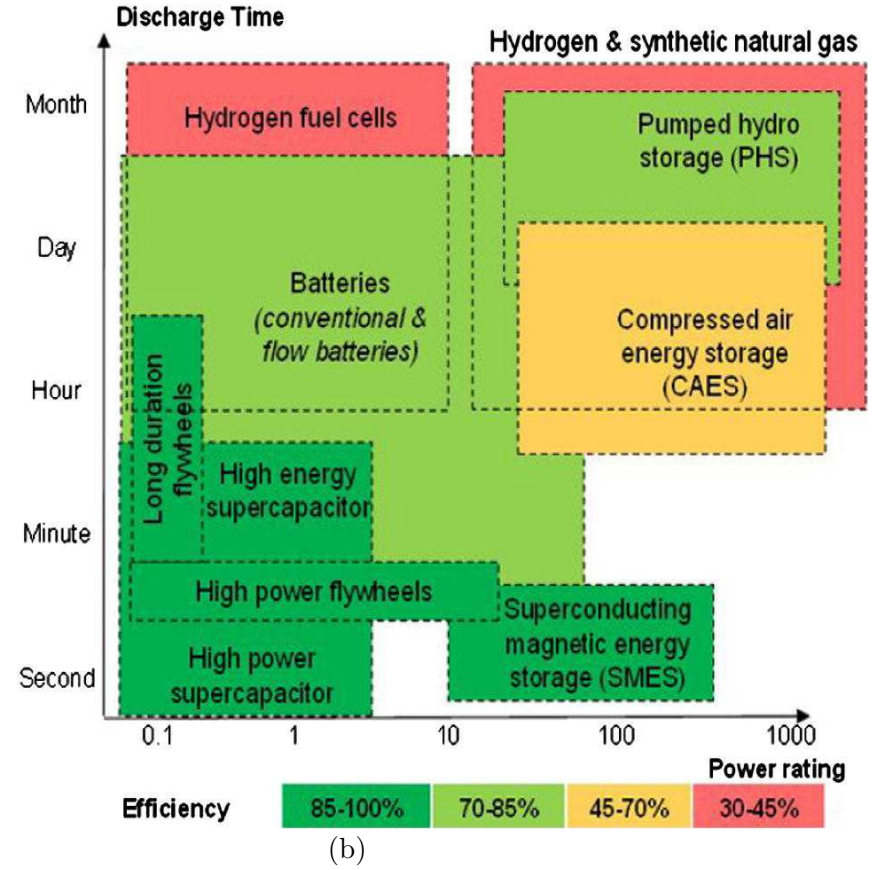

(b)

Figure 2.5 – ESS (a) application requirements and (b) operational parameters (4).

2.4 Thermo-mechanical systems for long-term energy storage

2.4.1 Compressed Air Energy Storage

Long-term energy storage is usually achieved through PHES (Pumped Hydroelectric Energy Storage) or CAES because of their lower cost per kWh, lower self-discharge rates and technological maturity (54, 55). The charging phase in CAES consists in the compression of ambient air, in a compressor or set of compressors, the air is subsequently cooled in a cooler or TES (Thermal Energy Storage) and stored at high pressure. During discharge the pressurized air is heated, in a heater and/or TES, afterwards it expands, generating energy and is, finally, released to the environment. Past CAES plants use natural gas to heat the compressed air before each turbine, as shown in the schematics for the CAES plant installed in Huntorf, Germany, Fig. 2.6. More recent designs for CAES systems recover the heat of compression instead of burners to increase system efficiency (5, 56, 57).

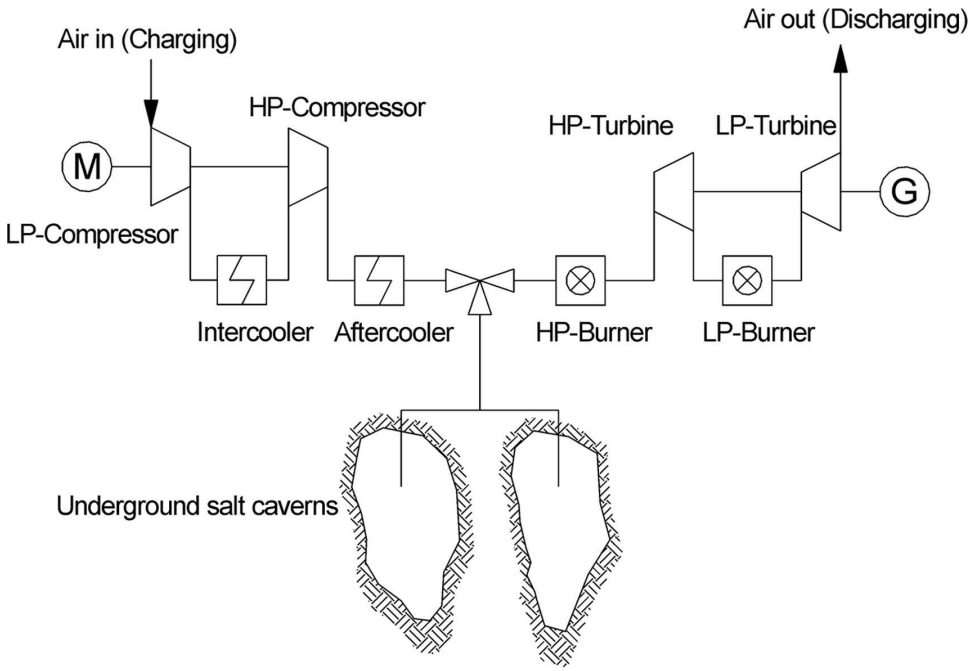

Figure 2.6 – Schematics of the CAES plant in Huntorf, Germany (5).

CAES systems can be classified as Adiabatic, Diabatic and Isothermal CAES (usually referred to as A-CAES, CAES and I-CAES) depending on how air is stored and heat is dissipated. In an A-CAES system the heat of compression is stored in a TES to be recovered during the discharging process, while in the diabatic CAES, such as the one on Fig. 2.6, this heat is lost to the environment and a heat source must be available for the expansion process. I-CAES has an nearly isothermal compression and expansion processes, increasing round-trip efficiency and lowering cost (58). Both A-CAES and I-CAES are developments in CAES to increase its competitivity as an energy storage system.

One of the main disadvantages of CAES is their relatively low energy density, as the energy is stored in the form of pressurized air. As a consequence the required volume for bulk energy storage with CAES is high, increasing the capital cost of pressure vessels and are usually viable for bulk energy storage when associated with underground caverns or aquifers (59). This imposes an important restriction for the use of CAES, even higher than for PHES, especially when combined with wind or solar energy as the installation region must have the adequate conditions for energy generation (solar and/or wind resources) and also have natural formations allowing high pressure air storage (60). Figures 2.7 and 2.8 shows the possible sites, in red, for installation of hybrid renewable energy-CAES systems in Iran (6) and China (7), respectively.

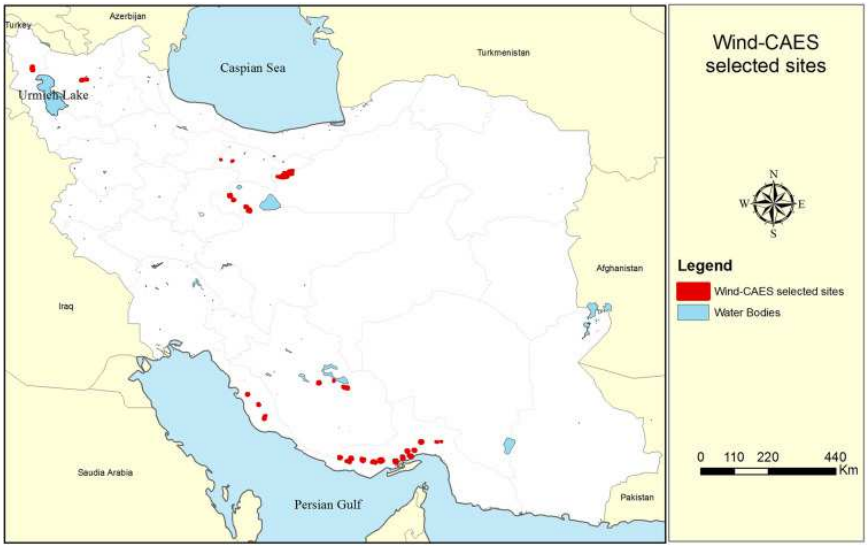

Figure 2.7 – Potential hybrid Wind energy / CAES installation sites (in red) in Iran (6).

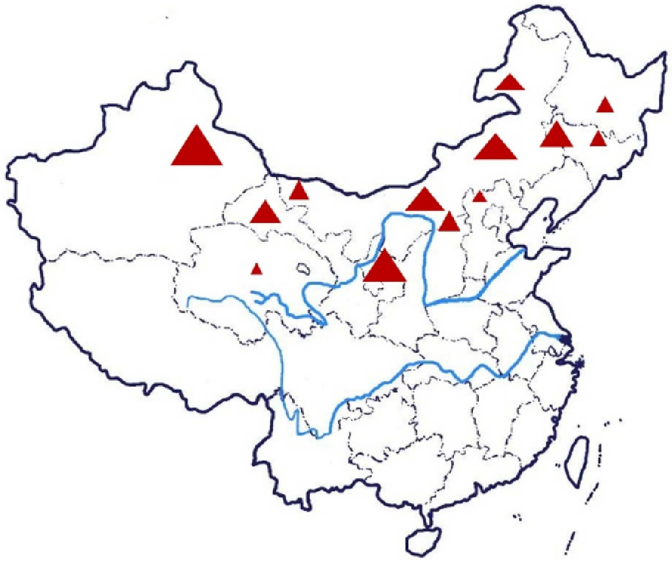

Figure 2.8 – Potential hybrid Wind-Solar-CAES installation sites (in red) in China (7).

The study of Figures 2.7 and 2.8 indicates the limitations imposed by the combination of CAES with photovoltaic and/or wind energy systems. It should be noted that the restriction for installation in China was higher than for Iran, as it considered hybrid Wind-Solar-CAES systems. If only Wind-CAES systems were considered there would be more alternative sites, specially on the southeast region of China (7).

2.4.2 Liquid Air Energy Storage

LAES (Liquid Air Energy Storage) was developed as an alternative to CAES. Higher energy densities can be achieved because air is stored in liquid state at cryogenic temperatures, avoiding the geographical constraints imposed to CAES and PHES (61). During the energy storage process, excess energy is used for the liquefaction process, which consists in the compression of ambient air followed by cooling and expansion in an expansion valve. After that, air reaches the storage tank, where it is kept around ambient pressure and cryogenic temperatures (circa 77 K). The fraction of that has not been liquefied returns and is used to cool the air leaving the compressor. After this, the returning air is mixed with ambient air and completes the cycle. During the discharging phase, liquid air is pumped by a cryogenic pump, and heated (either with heat stored from the liquefaction process or an external source) before entering the turbine (62). For most LAES systems, multiple stages are needed for both the compression and expansion processes. The schematics for a simple LAES system is shown in Fig. 2.9. Most LAES systems employ several mechanisms, such as heat and cold recovery and by-pass turbines, to increase system efficiency (29, 63).

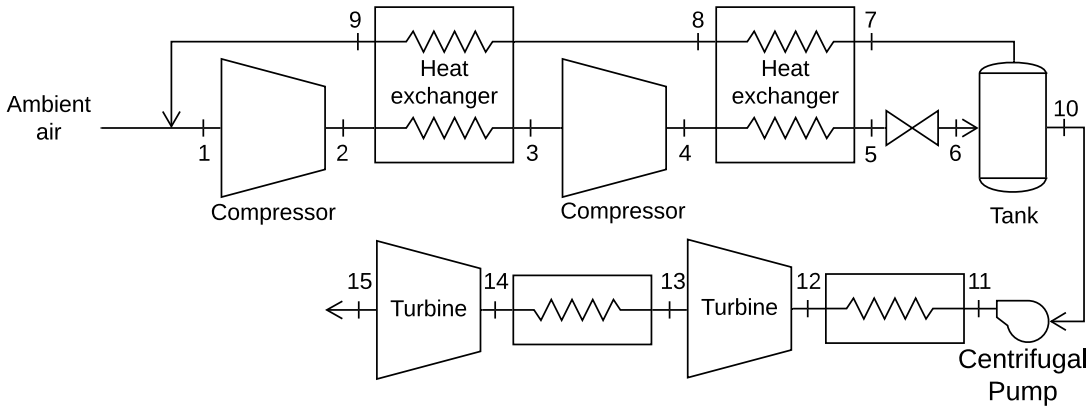

Figure 2.9 – Schematics of a LAES plant.

LAES are on an earlier stage of deployment but already have been installed at pilot and commercial scales in the United Kingdom reaching up to 5 MW (29). One of the main challenges for LAES is related to cost, that is mostly comprised of investment on the charging/liquefaction process that can be over three times the investment with the discharging process components or the storage tank (64, 65, 66). LAES are also significantly affected by off-design conditions, a study on LAES for three combinations of arbitrage, STOR (Short-Term Operating Reserve) and fast reserve services and found loss in component efficiency of up to 50% and in the round-trip efficiency of up to 30% (67).

2.4.3 Compressed CO_2 Energy Storage

Recently, new ESS, known as CCES (Compressed CO_2 Energy Storage) and PTES (Pumped Thermal Energy Storage), have been proposed as alternatives to CAES. CCES operates with two tanks, a high pressure tank and a low pressure tank. During energy storage CO_2 from the low pressure tank is compressed and cooled before entering the high pressure tank. During energy discharge the CO_2 from the high pressure tank is heated and expanded before being cooled down again before returning to the low pressure tank(8). Figure 2.10 illustrates the schematics and T-s diagram for a CCES system (8).

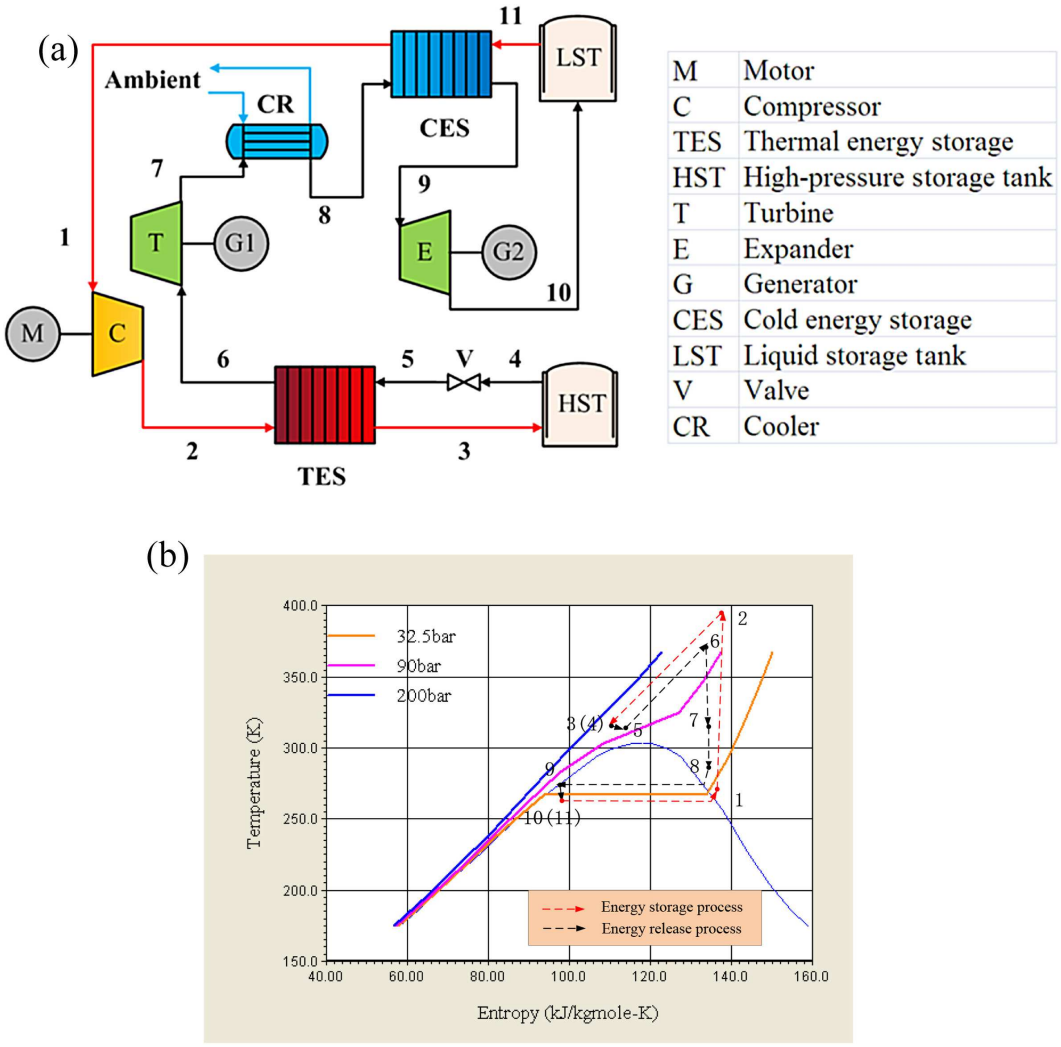

M	Motor
C	Compressor
TES	Thermal energy storage
HST	High-pressure storage tank
T	Turbine
E	Expander
G	Generator
CES	Cold energy storage
LST	Liquid storage tank
V	Valve
CR	Cooler

Figure 2.10 – Schematics of a CCES system (8)

CCES operates with pressures ranging from 25 to 200 bar, whereas CAES operates between ambient pressure and 80 bar, and is still on an earlier stage of development. CCES has been evaluated analytically achieving an energy density of 8 Wh/L, higher than CAES, and a round-trip efficiency ranging from 56 up to 71%, slightly higher than that for LAES systems (8, 68, 69, 70).

2.4.4 Pumped Thermal Energy Storage

The PTES is composed of a compressor, an expander and two thermal storage vessels, one hot and the other cold. During energy storage it works as a heat pump, transferring heat from the cold to the hot thermal storage, and during energy generation it operates as a heat engine. PTES is on a more advanced stage of development, with the first grid-scale demonstration plant, with a capacity of 150 kW / 600 kWh, in operation in Newscastle, UK (32). Figure 2.11 shows a basic schematic for PTES and its T-s diagram.

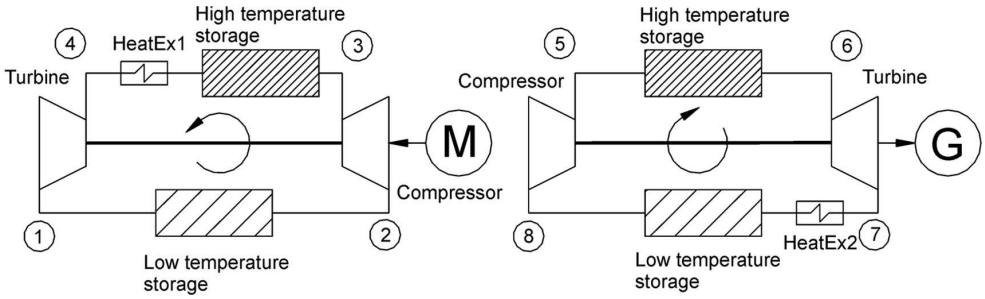

(a)

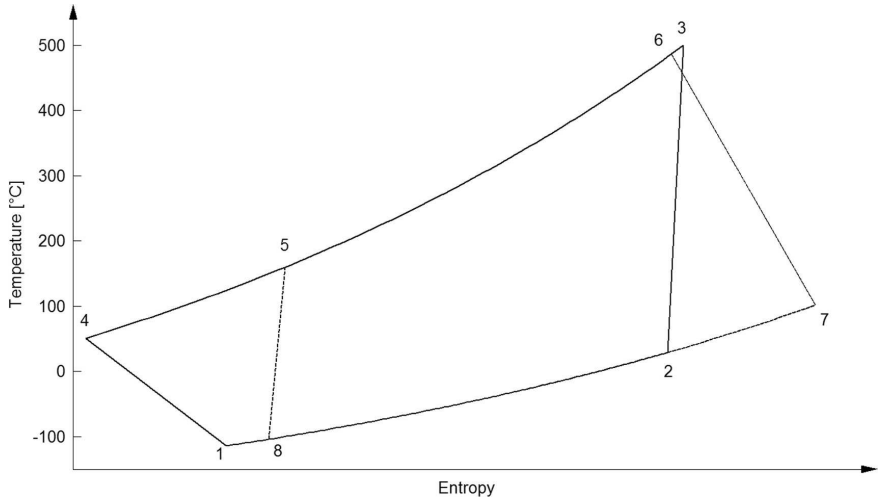

(b)

Figure 2.11 – (a) Schematics and (b) T-s diagram for the PTES system (charging in the left and discharging in the right) (5).

Reported values for the round-trip efficiency of PTES systems range from 40% up to 130%, mostly working with heat sources of up to 450 K (32, 71, 72, 73).

2.5 Hybrid Energy Storage systems

Another solution for the expansion of applications for energy storage is the integration of two or more energy storage technologies to supply a wider array of applications. In hybrid energy storage systems one storage is used as the bulk energy storage, with lower self-discharge rate and lower energy-specific cost, while the other storage is dedicated to transient and power quality applications, with low response time and high cycle lifetime (22, 74). Some examples of possible hybrid systems are CAES-SMES, PHES-FESS and BESS-supercapacitor (23). The increased complexity in the design process results in a system with an increased lifetime, lower cost and lower response time. Hybrid systems are particularly suitable for microgrid applications (74).

2.6 Conclusions

This chapter reviewed the background for energy storage systems, defining the main requirements as a function of energy grid application. This was followed by the presentation of the main classifications of ESS, their key performance parameters, and a brief introduction to the main bulk energy storage systems.

Increased energy demand and the expansion of intermittent energy sources in several national grids has increased the demand for bulk scale energy storage systems. The most mature bulk scale energy storage systems, PHES and CAES, have geographical constraints which also imply higher energy loss with transmission. More recent research have proposed a variety of new energy storage systems as alternatives to the traditional bulk storage systems, the most promising being LAES, CCES and PTES.

3 Organic Rankine Cycle

The ORC (Organic Rankine Cycle) was developed to allow the extraction of power from low-temperature heat sources, such as geothermal, solar and biomass. The ORC is very similar to the traditional SRC (Steam Rankine Cycle) but with the substitution of water by an organic fluid (usually hydrocarbons or refrigerants). The use of water as a working fluid in a Rankine cycle leads to multistage turbines with wet expansion, increasing costs and making it infeasible for low-temperature energy sources (14). Organic fluids have been considered as working fluids instead of water based on two aspects. First, the use of organic fluids adds another degree of freedom during the design phase, allowing a more flexible design process that matches more closely the heat source and heat sink temperature profiles. Secondly, the development of Steam Rankine cycles for low to medium power with high efficiency and at a feasible cost can be challenging, requiring multiple stages and complex plant layouts (14, 75).

Cycles based on organic fluids have been studied for several years, a first patent dating to 1832. Despite the age of the system, research has been encouraged by several events over time, such as the oil crisis in the 80s and, most recently, the increased interest in renewable energy sources (10, 13). The working fluids used in the ORC have lower boiling temperatures and pressures, reason for the higher potential of application for low-grade heat sources. Another advantage is that the working fluids suitable for the ORC usually present either an isentropic or positive sloped saturation vapor curve, resulting in a dry expansion, which reduces expander wear and, consequently, maintenance costs (9, 13). The comparison of the T-s diagram for water and some common organic fluids is shown in Figure 3.1.

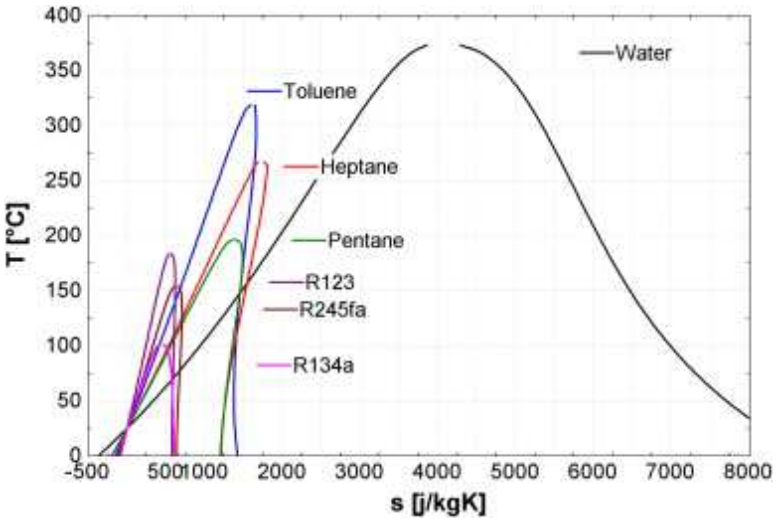

Figure 3.1 – Comparison of the T-s diagram of water and some organic fluids (9).

The skewed characteristic of the T-s curve for organic fluids indicate that the evaporation process requires less heat than water. It can also be seen that R-134a, R-245fa and R-123 have isentropic vapour saturation curves while Toluene, Heptane and Pentane have a positive sloped saturation curve, which means all of the fluids shown have a dry expansion.

In an ORC, the working fluid is pumped and goes through an evaporator before entering the expander as superheated vapor, generating power, and is then cooled in a condenser before reentering the pump, as represented on Figure 3.2.

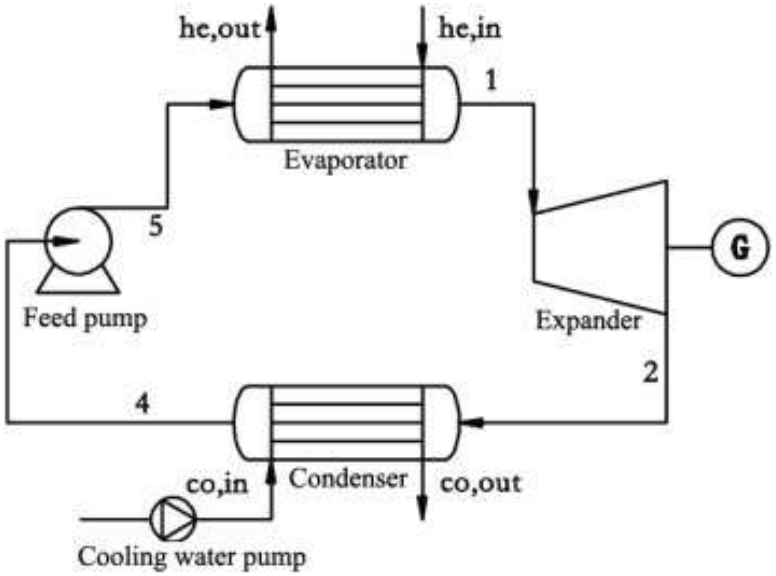

Figure 3.2 – Organic Rankine Cycle schematic representation (10).

3.1 Working fluid properties

Several factors must be taken into account when choosing the working fluid and they can be divided in safety, environmental and thermo-physical properties, as presented in Fig. 3.3.

The evaluation of some properties is rather straight forward. It is desired that the fluid has higher density, as this results in smaller components; lower viscosity, which results in lower friction; lower cost; and fluid availability. ORCs are usually more efficient when the critical temperature of the fluid is close to the maximum temperature of the heat source. The slope of the evaporation line is also important, as discussed at the beginning of the chapter. Researches indicate that, for low-temperature heat sources, isentropic and dry fluids outperform wet fluids (13, 76). The safety of the fluid can be obtained by their safety classification as established by ASHRAE, which expresses both toxicity and flammability. The classification is composed of two digits, the first refers to toxicity and goes from A, representing toxicity not identified at concentrations lower than or equal to

Figure 3.3 – Main characteristics of organic fluids (11).

400 ppm, to B, toxicity identified for concentrations below 400 ppm, and the second to flammability, from 1 to 3, with 1 representing no flame propagation at ambient conditions (which ASHRAE considered to be 21 °C and 101 kPa), 2 have lower flammability limit and 3 are highly flammable (A2L and B2L are lower flammability refrigerants with a minimum burning velocity under 10 cm s^{-1}) (77), Fig. 3.4 illustrates this classification.

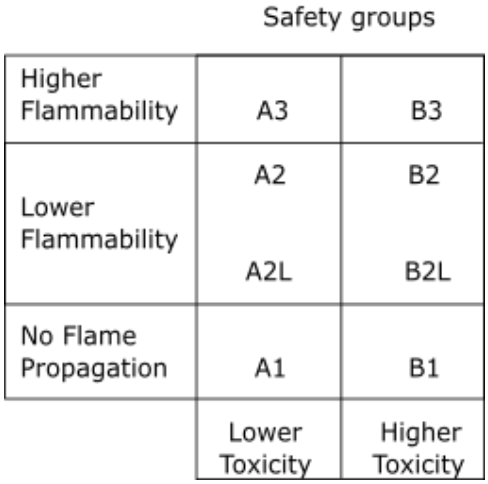

Figure 3.4 – ASHRAE Standard 34 Safety Classification groups (12).

The environmental safety of the fluid is mainly evaluated considering the effects on the ozone layer and on climate change with the ODP (Ozone Depletion Potential) and GWP (Global Warming Potential), respectively. The ODP is defined as the ratio of the impact of the chemical component on ozone to the impact of R-11 (78). The GWP

was developed to allow comparisons of the global warming impacts of different gases. Specifically, it is a measure of how much energy the emissions of a ton of the chemical component will absorb over a given period of time relative to the emissions of one ton of carbon dioxide (CO_2). The larger the GWP, the more the given gas warms the Earth compared to CO_2 over that time period. The time period usually used for GWPs is 100 years (79).

3.2 Expanders

The expander selection is a function of the working fluid, operating conditions and range of power output and can be classified in two groups: volumetric and velocity expanders (13). Volumetric expanders (vane, scroll, screw and piston) are suitable for low to medium scale systems (up to 200 kW) whereas velocity expanders (axial and radial turbines) for medium to large scale (over 500 kW), with a maximum power capacity of 10 MW (13, 75, 80, 81).

Volumetric expanders can be classified as either rotary or reciprocating. Among the volumetric rotary expanders, the screw expander is one of the most used, which can generate up to 5 MW, but being more suitable for the range of 50 kW to 1 MW, as volumetric expander cost increases considerably for higher power rates (81). For higher power capacity, axial turbines are better suited to work with high mass flow rates and low-pressure ratio while radial turbine is more suitable for systems that have low mass flow rates and high-pressure ratios. Therefore, the radial turbines are usually preferred over axial turbines in ORC applications (82). Figure 3.5 illustrates the classification of expanders based on power capacity, type of expander, stages and pressure ratio.

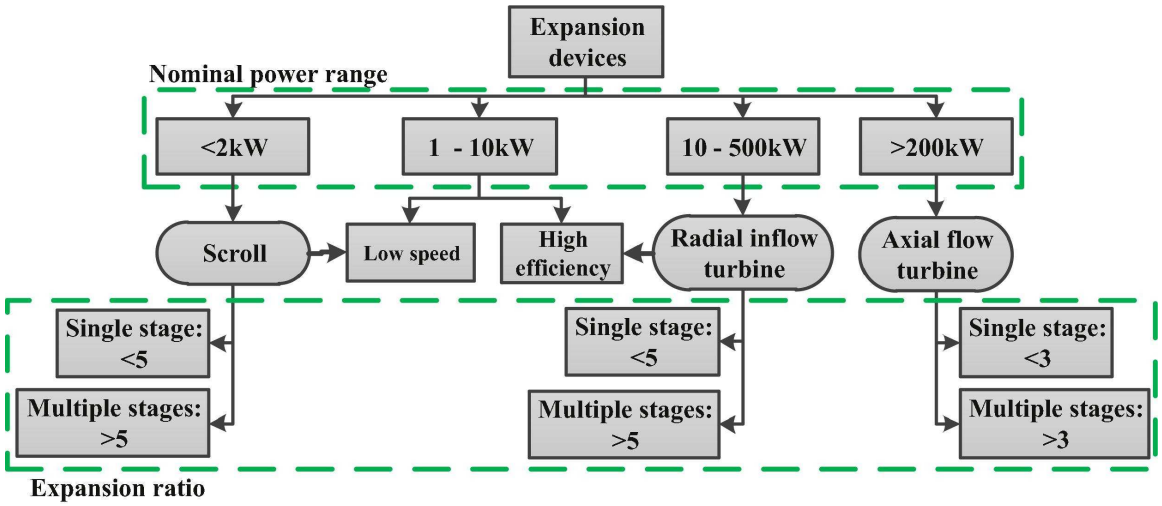

Figure 3.5 – Expander classification based on power capacity, expander type, number of stages and pressure ratio (13)

3.3 Organic Rankine Cycle classification

The ORC can be classified as subcritical or supercritical (also called transcritical) depending on the number of phases during the heating of the working fluid before entering the turbine. In a subcritical ORC the working fluid is heated in an evaporator passing through a two-phase state and in the supercritical ORC the working fluid is directly pumped up to a supercritical pressure. It is then heated in a vapor generator, bypassing the two-phase region (83). Research on supercritical ORC is relatively recent, but it has outperformed the subcritical ORC in most comparative studies, mostly because of the higher mean temperature in the heating process. However, the work of (84) supports that supercritical ORC would only operate properly for large differences between inlet and outlet temperature of the heat source and the work of (85) obtained maximum net work output for near-critical conditions instead of supercritical conditions. The work presented by (86) also indicate supercritical ORC only for heat source temperatures over 240 °C.

The Organic Rankine Cycle can also be classified based on the class of the working fluid (hidrocarbons, fluorocarbons, siloxanes or a mixture of organic fluids) each suitable for different thermal energy source (75). The incorporation of a fluid mixture in an ORC design requires the selection of the fluids to be mixed and the fractions of each fluid on the mixture. Working fluid mixtures increases the complexity of system design, whilst also increasing flexibility and might improve heat transfer because of their non-isothermal phase change (87, 88). For example, (89) realized an experimental study comparing two ORC, one with pure R-245fa and a second with a mixture of R-245fa and R-134a, with heat source temperatures between 80 °C and 120 °C and observed that the ORC with working fluid mixture generated more power for the lower temperatures (from 80 °C and 100 °C), but it was lower for 120 °C, concluding that working fluid mixtures could be more suitable in applications with higher temperature fluctuation. The range of applications for ORC for varying scales and heat source temperatures is illustrated in Fig. 3.6.

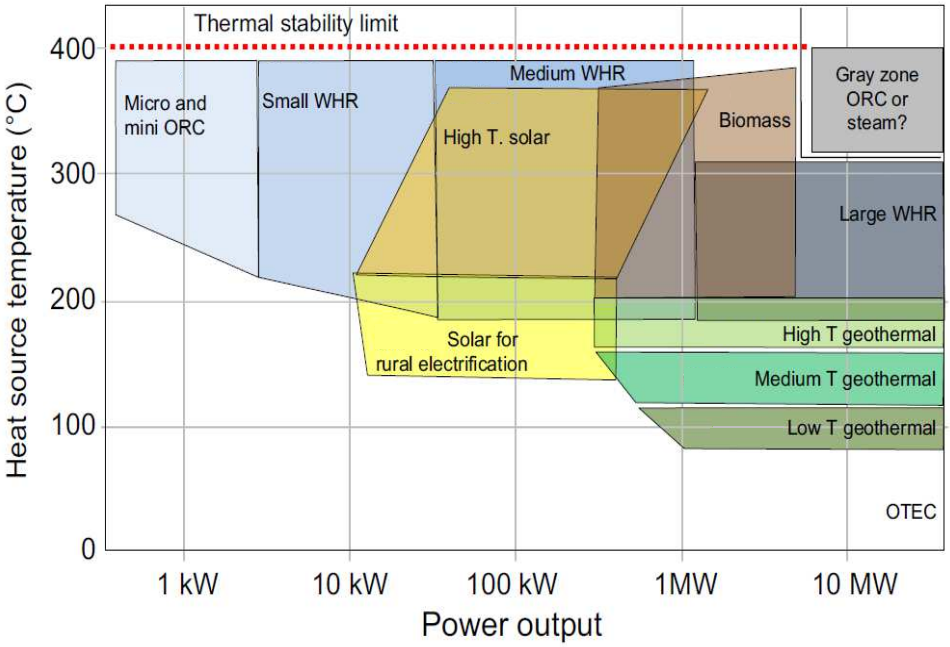

Figure 3.6 – ORC applications as a function of heat source temperature (°C) and power output (14).

ORC applications can be divided in Waste Heat Recovery (WHR), Biomass, Solar, and Geothermal ORC. Systems with power lower than 1 kW still have low efficiency, mostly because of the expander (14).

3.4 ORC design

The high number of real and theoretical working fluids suitable for the operation and cycle topologies increases the flexibility of ORC design to operate in a wide variety of applications (90). However, this increased flexibility also results in a higher number of decision parameters such as composition of the organic fluid (pure or mixed), working fluid selection, determination of the thermodynamic states and selection of type of ORC (Sub-critical or transcritical). Several studies have been developed on the design of ORC for different applications with focus on different aspects, mostly focused on working fluid and expander (91). The overall ORC design and optimization can be divided in three phases (1) problem analysis, (2) working fluid and cycle selection and (3) system optimization, which are often carried out iteratively to achieve an optimal design configuration and operation. During the first phase the technical constraints, environmental and safety requirements are used to obtain a list of possible working fluids, components selection and possible plant layouts. The selection of working fluid and cycle is usually carried out through an enumerative approach to simplify the selection process. An optimization process can be carried out for each combination of fluid and plant layout (14). The design process is illustrated in Fig. 3.7.

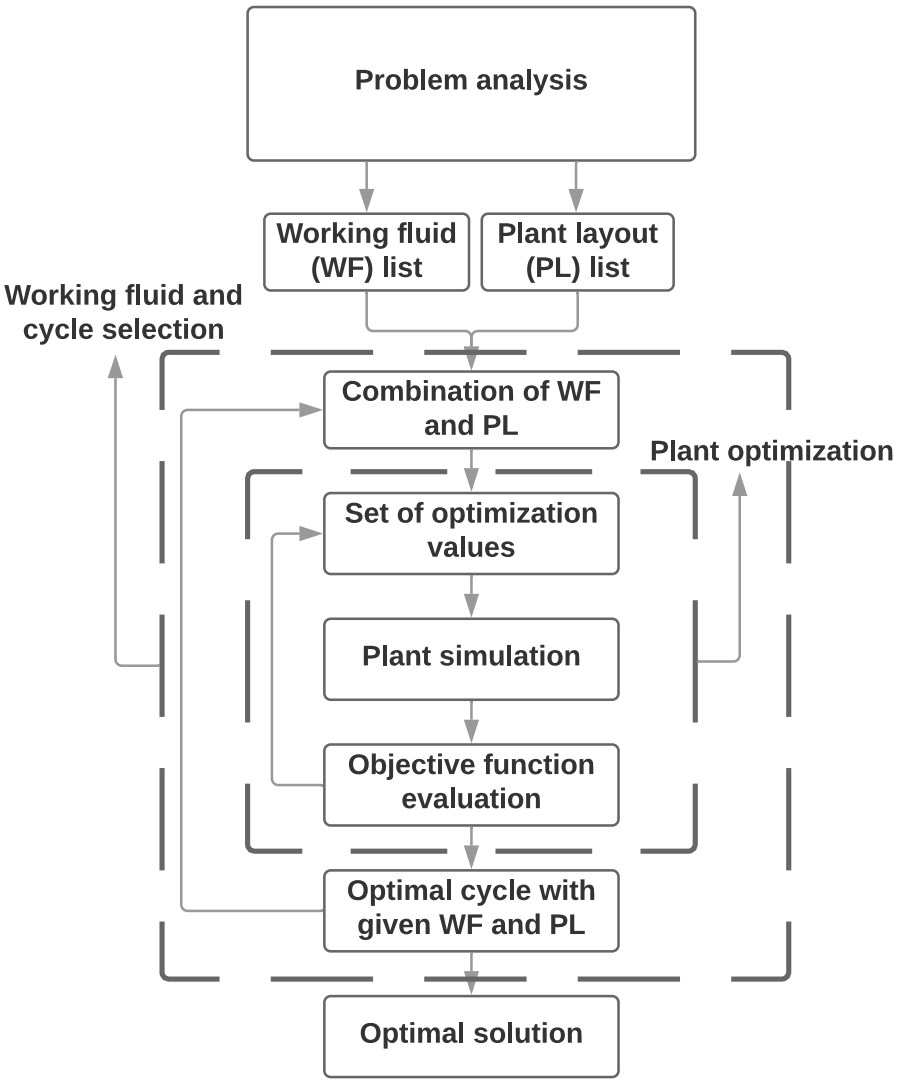

Figure 3.7 – ORC design and optimization process (Adapted from (14))

Based on system parameters and requirements (operational temperature and pressure range, cost, technical maturity, environmental and safety aspects) a subset of organic fluids is selected for analysis. While subcritical cycles are the most common layout, they are not the optimal solution for all applications and adequate variations of the system must be evaluated, e.g. supercritical ORC plants are more suitable for heat sources with variable temperature. The same must be observed regarding system components such as type of expander and use of recuperators (14).

The optimization of an ORC requires the definition of the objective function, i.e. determine a parameter to be maximized or minimized, the optimization variables, the models for the plant components and the optimization approach and algorithm. The objective functions for ORC can be divided in two main classes (1) maximize performance (10, 11, 19, 92); and (2) minimize cost (13, 33, 76), which can also be combined in a multi-objective optimization (14, 93, 94, 95). The most common performance indicators

for optimization are net work output, first and second-law efficiency which, usually, have the same trend in the optimization process (14, 92, 94, 96). The objective function for cost minimization is usually more complex as it requires reliable cost correlations, heat transfer coefficients and expander design, but represent a crucial aspect of the plant. The main parameters used for cost minimization are the specific cost and the LCOE (Levelized Cost of Electricity), with the latter being the most complex. The specific cost is defined as the ratio of total capital cost of the plant over the net power output. The LCOE can be defined as the ratio of the sum of the early costs of the system (capital, operation, management costs and monetary incentives) over the yearly energy production for the plant life time (14, 97, 98, 99).

3.5 Conclusions

This chapter reviewed the Organic Rankine Cycle, from applications, general properties of the organic fluids and system design. ORC have been widely used as an alternative to steam Rankine cycles in applications with low-grade temperature sources, such as geothermal, solar and waste heat recovery, as it usually results in simpler, cheaper and more efficient system. The variety of possible working fluids coupled with variations in cycle topology allows the ORC to be used in a wide range of applications. The design of ORC systems consists in the development of a list of possible fluids and topologies as a function of the application and evaluation of each of the possible combinations.

The study of the ORC technology indicates that application of ORC components to energy storage is suitable for small to medium scale systems, as current power output ranges from 1 kW to 10 MW. The application of ORC for heat recovery also indicates the potential of energy storage systems based on ORC for hybridization with other energy storage systems, specially those that already use ORC systems to improve efficiency.

4 Organic fluid potential as an energy storage medium

4.1 Introduction

Organic fluids have been widely used as a working fluid in systems for energy generation and some research has been done on the use of these fluids on ESS. However, despite being used as a working fluid on ESS, no study has been found on the use of organic fluids as the storage medium.

The use of organic fluids can result in a system with a higher energy density relative to CAES, as it can store the fluid as a liquid, with higher density than compressed air, and at lower pressures. The lower pressures and operation outside cryogenic regions also indicate lower cost relative to CAES and LAES.

The objective of this chapter is to evaluate the potential of a generic ESS using an organic fluid as the storage medium. As discussed in the previous section, there are several alternative organic working fluids, including mixtures. Since this is an initial study on the application of an energy storage system only commonly used, in literature and industry, pure organic fluids were considered for the analysis. From the set of commonly used fluids a sub-set was selected based on safety and environmental impact. Finally, the potential of the fluids in this sub-set was evaluated and compared to compressed air and liquid air (fluids used in CAES and LAES, respectively).

4.2 Exergy density

As described in chapter 2, the energy density of an ESS, ρ_E, is defined as the net electric energy generated during system discharge per unit mass (kWh kg^{-1}) or per unit volume (kWh m^{-3}) , indicating the required amount of working fluid or storage volume, which is directly related to the storage cost.

The potential energy density can be obtained by evaluating the exergy density of the fluid. The exergy of a fixed amount of mass stored at a determined state is defined as the maximum possible work that can be obtained from the system through a reversible process from an initial state to the dead state (a reference state, usually environmental conditions) (100). The exergy density would then be the ratio of exergy per unit mass, which is equal to the specific exergy, or per unit volume. The specific exergy χ of a fluid at a stationary storage tank is given by Eq. 4.1

$$\chi = u - u_o + P_o(v - v_o) - T_o(s - s_o), \tag{4.1}$$

where u, v and s are the specific internal energy, specific volume and specific entropy, respectively, of the fluid at the tank and u_0, v_0, s_0, P_0 and T_0 are the specific internal energy, specific volume, specific entropy, temperature and pressure, respectively, of the fluid at the dead state. The exergy density in terms of mass $\rho_{\chi,m}$ and volume $\rho_{\chi,V}$ are given by Eqs. 4.2 and 4.3, respectively,

$$\rho_{\chi,m} = \chi \tag{4.2}$$

$$\rho_{\chi,V} = \frac{\chi}{v} \tag{4.3}$$

4.3 Cost analysis

As a preliminary study on the potential of organic fluids without considering the processes of generation and storage, this study will focus on the minimum cost of storing the organic fluid. The material and structure of the storage tank is similar to that of CAES and the investment cost is then the sum of the costs of the storage tank itself C_{st} and the cost of the fluid C_{fl}. As air is obtained from the environment for CAES, the only costs are with the storage tank.

The estimation of the storage tank capital cost can be achieved with the equipment module costing technique. This technique estimates the capital cost of an equipment based on the cost of similar systems, including direct (equipment cost at manufacturer, materials required for installation, labour required for installation) and indirect costs (project expenses, contractor fees, auxiliary facilities), and adjusted through multiplying factors to account for variations in material, operational pressure, type of equipment, capacity, etc (15). The bare module cost of the storage tanks, C_{st}, is given by Eq. 4.4 to 4.6 (15)

$$C_{st} = C_{0,st}\ [B_{1,st} + (B_{2,st}\ F_{M,st}\ F_{P,st})], \tag{4.4}$$

$$log(C_{0,st}) = [K_{1,st} + K_{2,st}\ \log V + K_{3,st}\ (\log V)^2, \tag{4.5}$$

$$F_{P,st} = \frac{\frac{P_{barg}\ D_i}{2\ S\ E - 1.2\ P_{barg}} + CA}{t_{min}}, \tag{4.6}$$

where V is the volume in m^3, P_{barg} is the pressure gauge in bar, D_i is the storage tank internal diameter, S is the maximum allowable tension of the tank material, E is the welded joint efficiency, CA is the corrosion allowance and t_{min} is the minimum tank thickness. If $P_{barg} < -0.5$, F_p must be taken as 1.25 and, if the calculated $F_p < 1$, than $F_p = 1$ it must be used. The internal diameter D_i is calculated based on the indicated diameter for pressures over 34.47 bar (500 psi) as a function of volume (101),

$$D_i = \sqrt[3]{\frac{3\ V}{4\pi}} \tag{4.7}$$

The coefficients for eqs. 4.4 to 4.6 are shown in Table 4.1, considering carbon steel is used as construction material.

Table 4.1 – Coefficients of the bare module cost equation (15, 16).

	$B_{1,st}$	$B_{2,st}$	$K_{1,st}$	$K_{2,st}$	$K_{3,st}$	$F_{M,st}$
Storage tank	2.2500	1.8200	3.4974	0.4485	0.1074	1.0

Usually the cost data available is from previous years and inflation must be taken into consideration for a proper cost estimation. The cost available from a time i, C_i, can be adjusted to a time j, C_j, with their respective cost indexes, I_i and I_j with Eq. 4.8

$$C_j = C_i \left(\frac{I_j}{I_i}\right). \tag{4.8}$$

There are several, periodically calculated, cost indexes that estimate the overall inflation combining a few factors. The CEPCI (Chemical Engineering Plant Cost Index) is one of the main cost indexes, available at monthly and yearly publications, composed of four sub-indexes (Equipment; Construction Labor; Buildings; and Engineering & Supervision) (102). The coefficients presented in 4.1 were obtained based on a survey of equipment manufactures from May to September of 2001, with an average CEPCI of 397, and must be updated with the use of current values of CEPCI (15).

4.4 Methodology

The first step in the analysis is the selection of the fluids to be evaluated. A set of 27 commonly used organic fluids was obtained based on the literature (10, 39, 76, 82, 92, 103, 104, 105). Then, the safety classification, or hazard statements when the classification was not available, was obtained and the fluids with high flammability or toxicity were rejected, resulting in a sub-set of 12 fluids (4, 106, 107, 108, 109, 110). Finally, the fluids were further filtered based on their environmental impact. The ODP for all fluids was zero or close to zero, so GWP was used as the only qualification factor. Fluids with GWP over 2,500 were excluded from this study, this limit was established in order to favor environmentally-friendly fluids whilst maintaining a reasonable number of fluids for the study. The main properties of these organic fluids are displayed in Table 4.2.

Table 4.2 – Properties of the evaluated organic fluids (17).

	Molar mass [kg kmol^{-1}]	T_{crit} [K]	P_{crit} [kPa]	ODP	GWP (100 yr)	Safety classification	Cost [USD/kg]
R-152a	66.05	386.41	4,520	0	124	A2	2.96*
R-134a	102.03	374.21	4,059	0	1,430	A1	4.78*
R-142b	100.50	410.26	4,055	0.07	2,310	A2	3.06*
R-365mfc	148.08	460.00	3,266	0	794	N.A.	6.68*
R-141b	116.95	477.50	4,212	0.120	725	A2	4.22*

* All prices were obtained from online marketplaces. Companies: Shendong Marvel, Arkool, Synthes technologies, Career Henan Chemical and Wenzhou Foreign Trade Industry.

The exergy density of the working fluids were evaluated in the state of saturated liquid for P ranging from 5% over the saturation pressure at ambient temperature to 5% under the critical pressure. The results were compared to the exergy density for compressed air with P ranging from ambient pressure up to 8,000 kPa and T equal to 330 K, based on average pressure and temperature values for CAES (111, 112, 113). The exergy density of liquid air was evaluated for a state of ambient pressure and a cryogenic temperature of 78 K. The values of P and T for compressed and liquid air were determined based on the most common operational conditions for CAES and LAES systems (5, 114, 115, 116, 117). The cost as a function of P and T was then calculated for storage tank volumes of 2, 4, 6, 8 and 10 m^3. The cost values for the pressure vessels were updated to 2019 using yearly values of the CEPCI (15, 102).

4.5 Results

4.5.1 Exergy density

Figures 4.1a and 4.1b show the specific exergy (in kWh m^{-3} and kWh kg^{-1}, respectively) of the evaluated working fluids and for compressed air (dead state set at P_o = 100 kPa and T_o = 298.15 K).

The exergy density of the evaluated working fluids in terms of volume were all higher than for compressed air. Among the evaluated fluids R-134a and R-152a showed higher potential, with exergy density around $5-6$ times higher than compressed air at the same pressure and even more than double the exergy density than those reported for operational CAES systems, for which air is stored at pressures ranging from $4-8$ MPa. In terms of mass the compressed air showed higher exergy density than all of the evaluated fluids, achieving values over three times higher than that for the R-152a, the organic fluid with the highest exergy density in kWh kg^{-1}. The exergy density for liquid air is 180 kWh m^{-3} and 0.21 kWh kg^{-1}, much higher than both the organic fluids and compressed air,

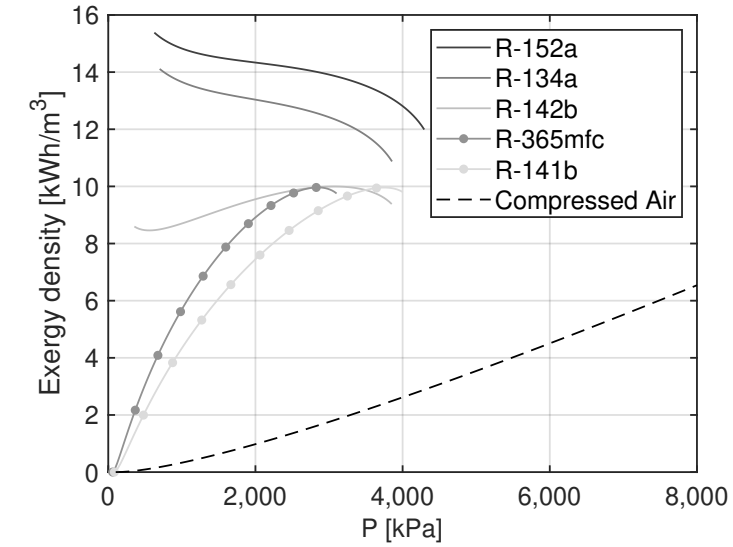

(a)

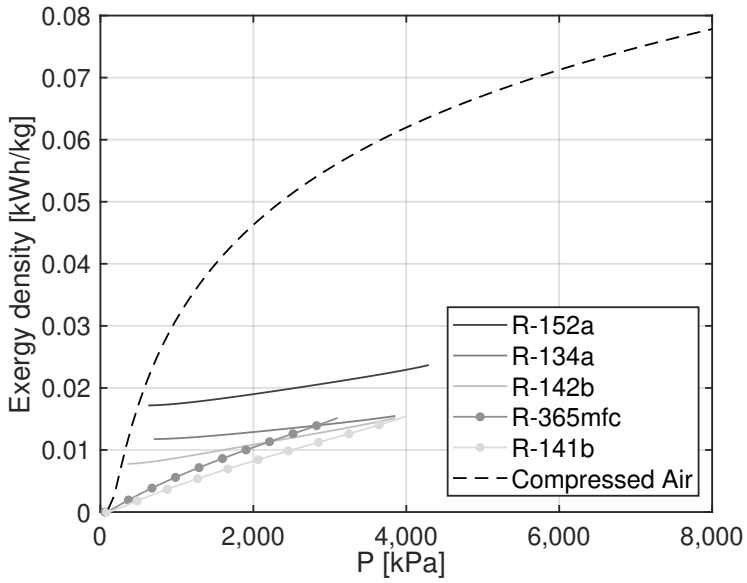

(b)

Figure 4.1 – Exergy density in terms (a) of volume (kWh m^{-3}) and (b) of mass (kWh kg^{-1}) as a function of pressure for the evaluated organic fluids and compressed air.

independent of the storage pressure.

4.5.2 Storage cost

The cost of the storage tank as a function of pressure and volume is shown in Fig. 4.2.

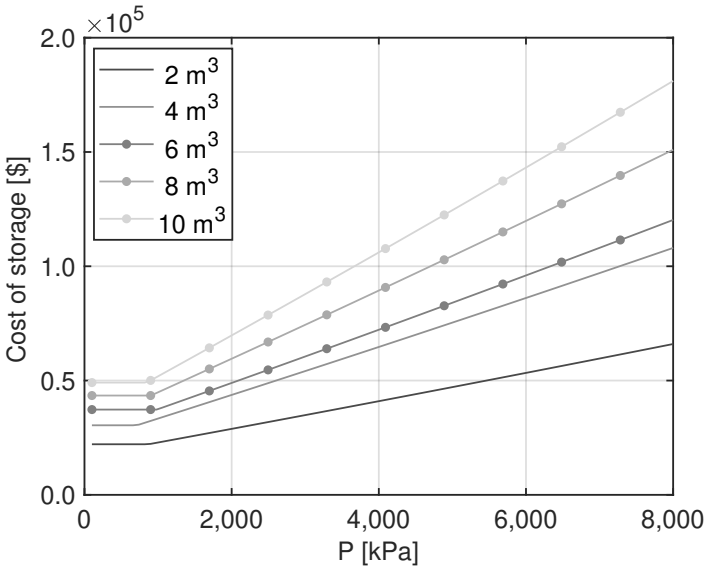

Figure 4.2 – Tank cost as a function of pressure for storage volumes of 2, 4, 6, 8, and 10 m^3.

The cost of the storage tank is constant for lower pressures, as there is a lower limit for the vessel thickness, before increasing linearly with pressure. In the previous subsection it was seen that the organic fluids had exergy density ranging from 8 to 16 kWh m^{-3}, up to pressures around 4,200 kPa, while air, at CAES operational conditions (around 8,000 kPa), has a maximum exergy density around 6 kWh m^{-3}, which is even lower than the values for the organic fluids at half the pressure. The cost of the tank for compressed air is then almost double the cost of the tank for organic fluids (considering they are operating close to their critical pressure) with around half of the exergy.

The cost of the storage system for the organic fluids is the sum of the storage tank and of the fluid itself. Equations 4.3 to 4.8, combined with cost of each fluid, were then used to estimate the total cost of the storage system (tank + fluid) for organic fluids, and the results are shown in Figs. 4.3a to 4.3e.

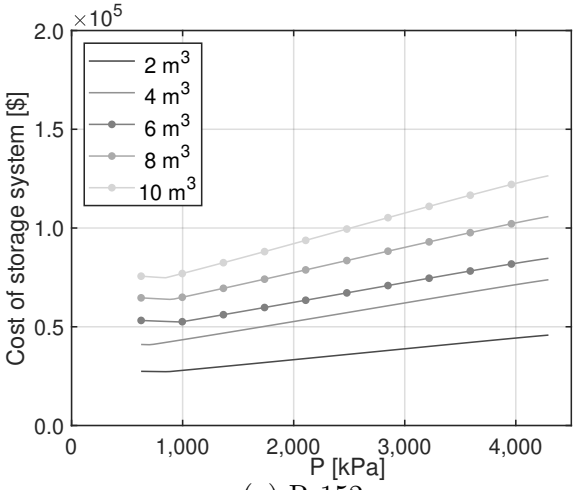

(a) R-152a

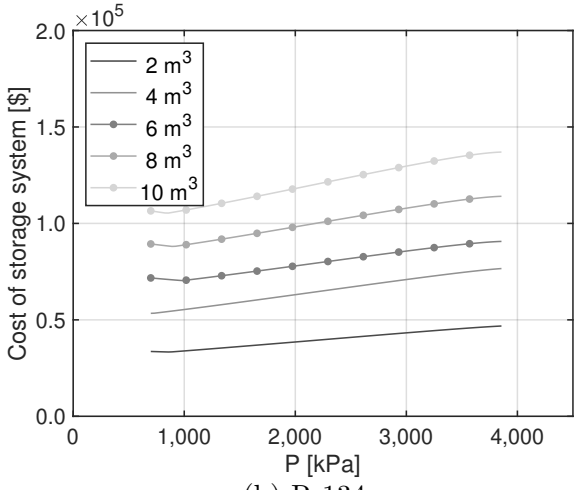

(b) R-134a

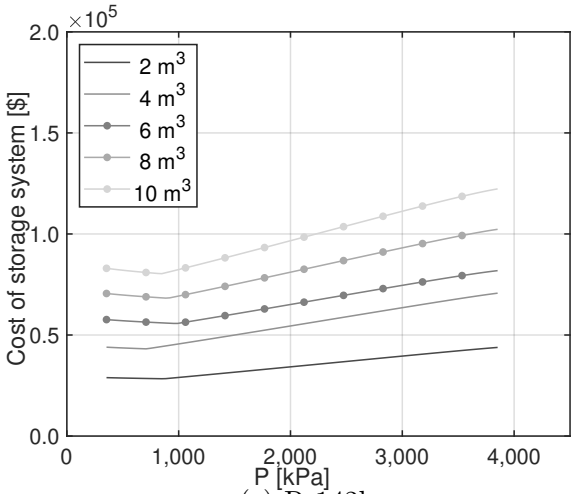

(c) R-142b

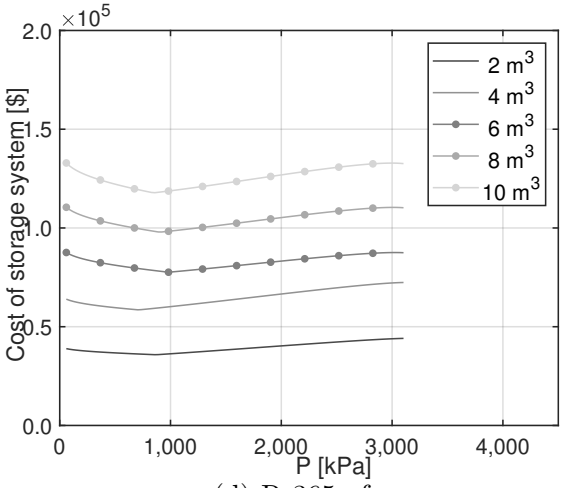

(d) R-365mfc

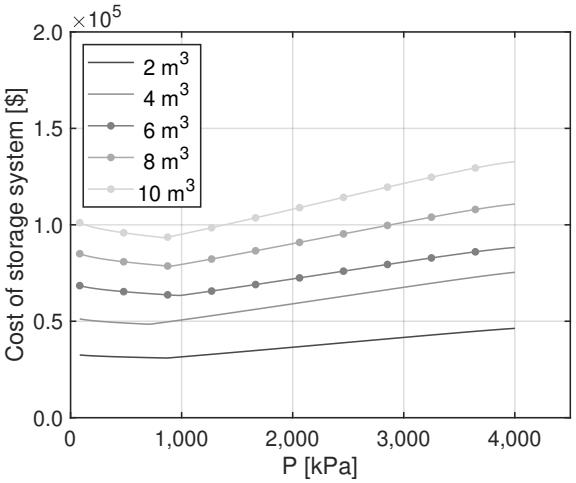

(e) R-141b

Figure 4.3 – Storage system (tank + fluid) cost as a function of pressure and volume (m^3) for the evaluated organic fluids.

The increase in cost due to the organic fluids represents only a small fraction of the overall cost of the storage system, remaining cheaper than the storage for compressed air at common CAES operational conditions. All fluids presented a similar behavior, in the region of low pressure, as the thickness was constant, the increase in pressure resulted in a reduction of the total fluid mass stored and, consequently, lower cost. Since higher pressures demanded higher tank thickness, there was an almost linear increase in the storage system cost. The difference in cost was more significant for higher volumes, with the cheapest energy storage system for R-142b and R-152a. The cost difference between storage systems with organic fluids and compressed air would be even wider for a complete energy storage system, as other component costs can be greatly influenced by operational pressure, such as heat exchangers.

The previous results discuss only the cost as a function of pressure and volume. Figs. 4.4a to 4.4e show the cost per unit of stored energy for the organic fluids and Fig. 4.4f

for compressed air.

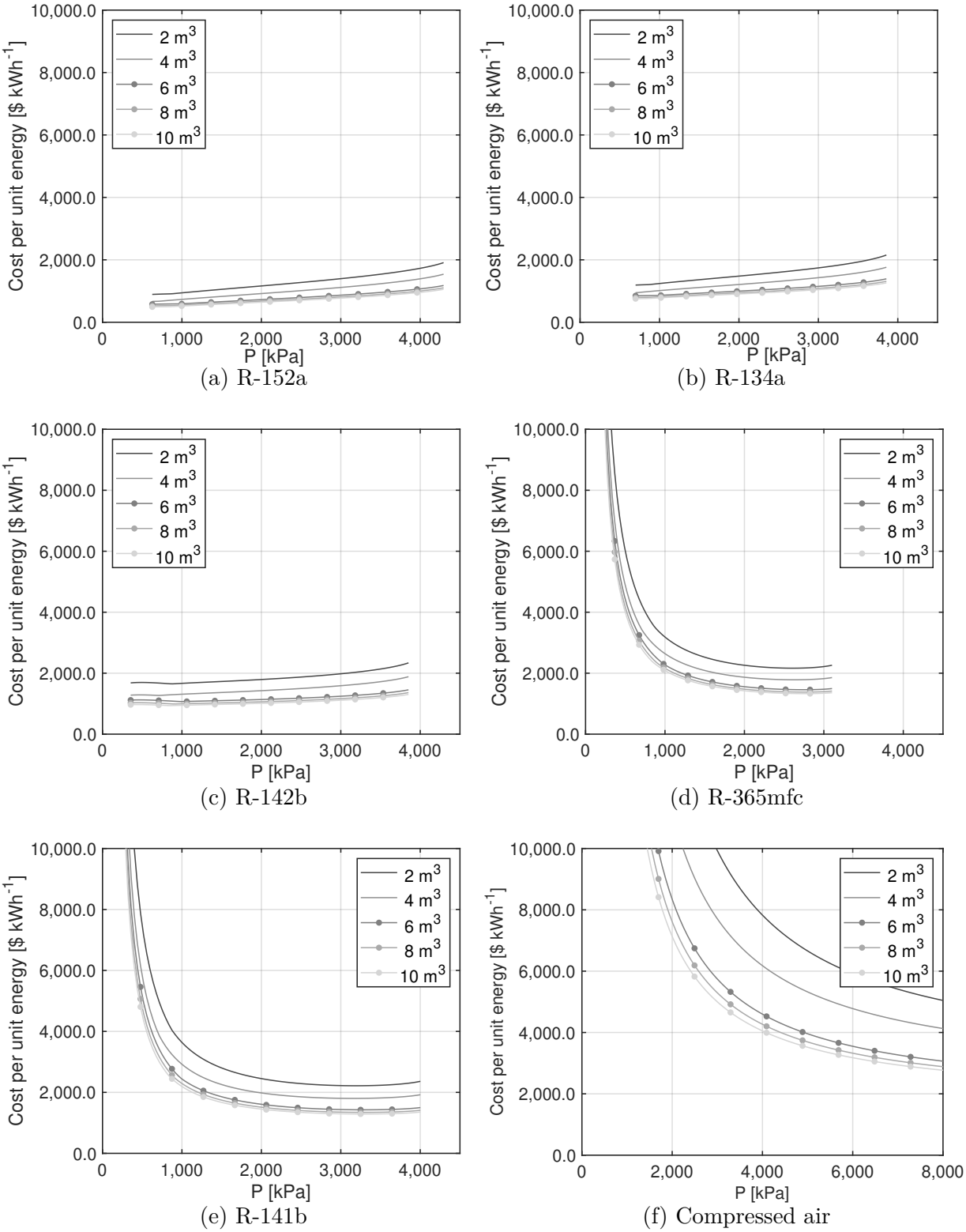

(a) R-152a (b) R-134a

(c) R-142b (d) R-365mfc

(e) R-141b (f) Compressed air

Figure 4.4 – Cost per unit energy as a function of pressure and volume (m^3) for the evaluated organic fluids and compressed air.

Despite the higher cost for the same volume, the cost per unit energy was lower

than compressed air for all of the evaluated organic fluids, mostly because of the higher exergy density of the organic fluids relative to compressed air. The cost per unit energy is the result of a combination of exergy density, fluid cost and specific volume. The fluids with the lowest cost per kWh of stored exergy over a wider range of storage pressures were R-152a, R-134a and R-142b, as a result of the combination of higher exergy density with low fluid cost. The cost per unit energy for these organic fluids at maximum pressure was only around 2,000 \$ kWh^{-1} and 1,200 \$ kWh^{-1} for storage volumes of 2 and 10 m^3, respectively, while the cost for compressed air were 5,045 and 2,769 \$ kWh^{-1} for the same storage volumes.

4.6 Conclusions

The objective of this chapter was to evaluate the potential application of organic fluids as energy storage mediums in technical and economic terms. Before analyzing any working fluid, a set of five working fluids was selected establishing as selection criteria their commercial maturity, safety hazards, and environmental impact. First, the technical potential of these fluids was evaluated in the form of their exergy density, i.e. the maximum work that can be obtained per unit mass and per unit volume of organic fluid. The exergy density of these fluids was calculated for storage at pressures ranging from 5% above their saturation pressure at ambient temperature to 5% under their critical pressure at the state of saturated liquid. The results were compared to the exergy density of air with storage pressures ranging from ambient pressure up to 8,000 kPa and to the exergy of liquid air at 78 K and ambient pressure (common storage conditions for CAES and LAES plants, respectively). The evaluated organic fluids showed exergy densities over five times the exergy density of compressed air for the same pressures, reaching even higher values when comparing to the exergy density of compressed air at 8,000 kPa. Their exergy density was still much lower than the exergy density of liquid air at 180 kWh m^{-3}.

The economic aspect of the organic fluid was first evaluated in terms of the capital cost of the storage system (cost of the storage tank and working fluid). The storage tank material is the same for both air and the organic fluids and its cost is a function of the tank volume and pressure. The cost of the storage system for organic fluids also includes the cost of the fluid. The cost was then calculated for the same range of operational parameters for the organic fluids and compressed air for storage volumes of 2, 4, 6, 8 and 10 m^3. The storage system cost was slightly higher than that of compressed air for the same pressures and around 33% lower when compared to CAES operational conditions, i.e. 8,000 kPa. The difference when considering the cost per unit exergy was even higher because of the higher exergy density, and, therefore, higher energy capacity, of the organic fluid tanks. The fluids R-152a, R-134a and R-142b had the lower cost per unit exergy, mostly due to their higher exergy density coupled with a lower fluid cost relative to the

other organic fluids. The organic fluids showed the potential to store more energy at a higher density (up to 15 kWh m^{-3} compared to 6 kWh m^{-3} of compressed air) and at a lower cost when compared to compressed air.

5 Evaluation of an energy storage system based on the Organic Rankine Cycle

5.1 Introduction

In this chapter a new type of energy storage system based on the Organic Rankine Cycle, therefore called ORES (Organic Rankine Energy Storage), with the storage of energy in the form of pressurized organic fluid, is proposed. The operation of the storage system with organic fluids allows for the storage of working fluid in the liquid state without a cryogenic liquefaction plant, therefore providing a high density energy storage system with lower installation costs.

5.2 System description

The ORES system operates as a closed system and needs two storage tanks, a High Pressure Tank (HPT) and a Low Pressure Tank (LPT), both of which store the working fluid in a saturate liquid-vapor mixture state. The operation of the system can be divided in two stages, energy storage and energy discharge.

5.2.1 Energy discharge

The energy discharge phase is illustrated in Fig. 5.1, where active lines of the cycle are represented in black, and inactive in grey.

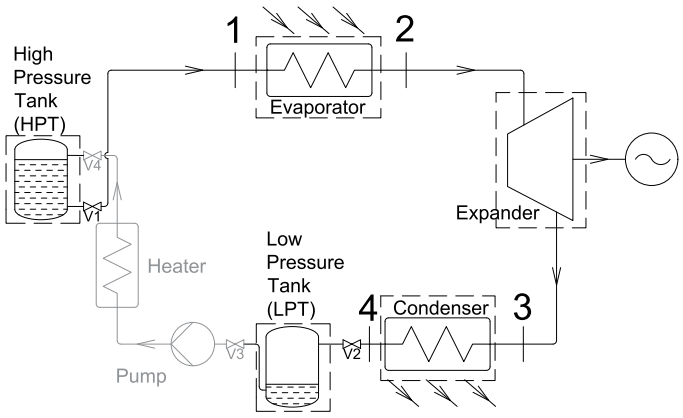

Figure 5.1 – Energy discharge phase (black - active line, grey - inactive line).

During discharging, saturated liquid flows out of the HPT, and goes into the evaporator before entering the expander. After passing through the expander, it is cooled to saturated liquid in the condenser. The heat per unit mass received in the evaporator

q_{Ev}, the specific work at the expander w_t, and the specific heat at the condenser q_C may be estimated from energy balances at the control volumes of each respective component, resulting in Eqs. 5.1, 5.2 and 5.3, respectively

$$q_{Ev} = h_2 - h_1, \tag{5.1}$$

$$w_t = h_2 - h_3, \tag{5.2}$$

$$q_C = h_3 - h_4, \tag{5.3}$$

where h_1, h_2, h_3 and h_4 are the specific enthalpies (kJ kg^{-1}) at the evaporator inlet, expander inlet, expander outlet and condenser outlet, respectively. Specific enthalpy h_3 is estimated from Eq. 5.4

$$h_3 = h_2 - \eta_t \ (h_2 - h_{3,s}), \tag{5.4}$$

where $h_{3,s}$ is the specific enthalpy for an isentropic expansion and η_t is the expander isentropic efficiency.

The mass flow rate during discharge, $\dot{m}_D$, can be obtained as a function of the required power in the expander $\dot{W}_t$, Eq. 5.5

$$\dot{m}_D = \frac{\dot{W}_t}{w_t}. \tag{5.5}$$

During the discharging stage, thermodynamic state of the HPT and LPT varies, which leads to a perturbation in the high (HPT and evaporator) and low pressure lines (condenser and LPT). Applying mass and energy balances for a control volume at the HPT results in Eqs. 5.6 and 5.7. Similar equations can be written for the LPT, Eqs. 5.8 and 5.9

$$\frac{d\ (m_{HPT})}{dt} = -\dot{m}_D, \tag{5.6}$$

$$\frac{d(U_{HPT})}{dt} = -\dot{m}_D \ h_{l,HPT}, \tag{5.7}$$

$$\frac{d\ (m_{LPT})}{dt} = \dot{m}_D, \tag{5.8}$$

$$\frac{d(U_{LPT})}{dt} = \dot{m}_D \ h_4, \tag{5.9}$$

where $h_{l,HPT}$ and h_4 are the enthalpy for the saturated liquid leaving the HPT and entering the LPT, respectively, m_{HPT} and U_{HPT} are the total mass and internal energy in the high pressure tank, m_{LPT} and U_{LPT} are the total mass and internal energy in the low pressure tank.

5.2.2 Energy storage

The charging process is illustrated in Fig. 5.2, with active lines in black and inactive in grey.

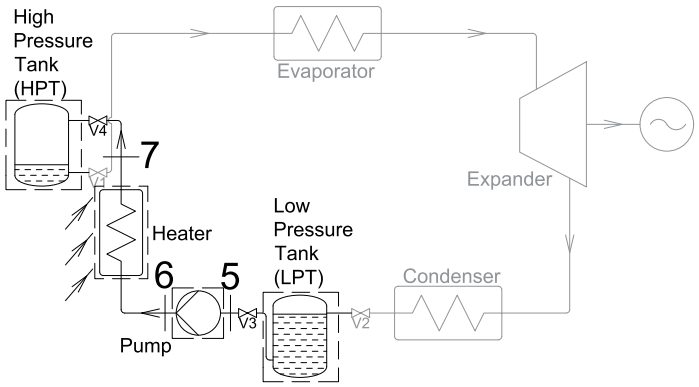

Figure 5.2 – Energy storage phase (black - active line, grey - inactive line).

Assuming the thermodynamic states of HPT and LPT at the beginning of the energy storage as known and considering that fluid leaves the storage tank as saturated liquid, specific enthalpy at state 6, h_6, can be found in terms of the state of the fluid at the pump inlet, h_5, the pump isentropic efficiency η_p, and the enthalpy for isentropic compression $h_{6,s}$, Eq. 5.10

$$h_6 = h_5 + \frac{h_{6,s} - h_5}{\eta_p}. \tag{5.10}$$

The specific work required by the pump w_p is obtained with an energy balance at the control volume of the pump, Eq. 5.11

$$w_p = h_6 - h_5. \tag{5.11}$$

The mass flow rate during charging, $\dot{m}_{Ch}$, can be obtained as a function of the power provided to the pump $\dot{W}_p$, Eq. 5.12

$$\dot{m}_{Ch} = \frac{\dot{W}_p}{w_p}. \tag{5.12}$$

After being pumped, the working fluid is heated before returning to the HPT. The heat per unit mass added during this process q_H can be obtained with an energy balance at the control volume of the heater, resulting in Eq. 5.13

$$q_H = h_7 - h_6. \tag{5.13}$$

The thermodynamic states also vary during the charging process. The energy and mass balances on the control volumes of both storage tanks result in Eqs. 5.14 to 5.17

$$\frac{d\ (m_{HPT})}{dt} = \dot{m}_{Ch}, \tag{5.14}$$

$$\frac{d(U_{HPT})}{dt} = \dot{m}_{Ch}\ h_7, \tag{5.15}$$

$$\frac{d\ (m_{LPT})}{dt} = -\dot{m}_{Ch}, \tag{5.16}$$

$$\frac{d(U_{LPT})}{dt} = -\dot{m}_{Ch}\ h_{l,LPT}, \tag{5.17}$$

where h_7 and $h_{l,LPT}$ are the enthalpy at the inlet of the HPT and the enthalpy of the saturated liquid leaving the LPT, respectively.

The heat required in the evaporator and in the heater is provided by two heat pumps, HP_1 and HP_2, respectively. The work consumed in the heat pump, W_{HP}, and the heat removed from the low temperature reservoir (ambient temperature), $Q_{L,HP}$, can be obtained from the definition of coefficient of performance and from an energy balance applied to each heat pump, Eqs. 5.18 to 5.21

$$W_{HP1} = Q_{Ev}/COP_{HP1}, \tag{5.18}$$

$$Q_{L,HP1} = Q_{Ev} - W_{HP1}, \tag{5.19}$$

$$W_{HP2} = Q_H/COP_{HP1}, \tag{5.20}$$

$$Q_{L,HP2} = Q_H - W_{HP2}, \tag{5.21}$$

The round-trip efficiency of an energy storage system can be defined as the ratio of produced electric energy during discharging and the electric energy consumed during system charging (4, 5). For the ORES system it can be calculated with Eq. 5.22

$$\eta_{RT} = \frac{W_t - W_{HP1}}{W_p + W_{HP2}}. \tag{5.22}$$

The energy density is here defined as the ratio of generated electric energy over storage volume (or mass) (4, 5, 62). The energy density of ORES, in terms of volume, ρ_{E_V}, and mass, ρ_{E_m}, are calculated with Eq. 5.23 and Eq. 5.24, respectively

$$\rho_{E_V} = \frac{W_t}{V_{HPT} + V_{LPT}}, \tag{5.23}$$

$$\rho_{E_m} = \frac{W_t}{m_{HPT} + m_{LPT}}. \tag{5.24}$$

5.3 Cost analysis

As a preliminary analysis it is desirable to evaluate the economic prospect of the system. To achieve this the CAPEX (Capital Expenditure) is estimated as the sum of their main components, namely turbine, pressure vessels, pump, working fluid and auxiliary equipment, Eq. 5.25. The remaining components usually represent a smaller contribution to system cost for similar systems (ORC and PTES) (118).

$$CAPEX = C_{fl} + C_{st} + C_t + C_{aux} + C_p. \tag{5.25}$$

Pump, turbine and storage tank costs are estimated with the bare module method (15). Pump cost is estimated as a function of power, pressure and material, Eqs. 5.26

to 5.28

$$C_p = C_{0,p}\ [B_{1,p} + (B_{2,p}\ F_{M,p}\ F_{P,p})], \tag{5.26}$$

$$\log\ C_{0,p} = K_{1,p} + K_{2,p}\ \log \dot{W}_p + K_{3,p}\ (\log \dot{W}_p)^2, \tag{5.27}$$

$$\log\ F_{P,p} = C_{1,p} + C_{2,p}\ \log P_p + C_{3,p}\ (\log P_p)^2, \tag{5.28}$$

where F_M and F_P are the material and pressure factors, respectively.

According to the bare module method the cost of the turbine can be obtained as a function of power, type of turbine and material, Eqs. 5.29 and 5.30 (15),

$$C_t = C_{0,t}\ F_{M,t}, \tag{5.29}$$

$$\log\ C_{0,t} = K_{1,t} + K_{2,t}\ \log \dot{W}_t + K_{3,t}\ (\log \dot{W}_t)^2. \tag{5.30}$$

Finally, the cost for pressure vessels can be estimated with Eqs. 5.31 to 5.33 (15)

$$C_{st} = C_{0,st}\ [B_{1,st} + (B_{2,st}\ F_{M,st}\ F_{P,st})], \tag{5.31}$$

$$\log C_{0,st} = [K_{1,st} + K_{2,st}\ \log V + K_{3,st}\ (\log V)^2, \tag{5.32}$$

$$F_{P,st} = \frac{\frac{P_{barg}\ D_i}{2\ S\ E - 1.2\ P_{barg}} + CA}{t_{min}}, \tag{5.33}$$

where V is the volume of the pressure vessel in m^3, P_{barg} is the pressure gauge in bar, D_i is the storage tank internal diameter, S is the maximum allowable tension, E is the welded joint efficiency, CA is the corrosion allowance and t_{min} is the minimum tank thickness. The coefficients for Eqs. 5.26 to 5.33 are shown in Table 5.1.

Table 5.1 – Coefficients of the bare module cost equation used to estimate pump, turbine and storage tank costs (15, 16, 18, 19).

	B_1	B_2	K_1	K_2	K_3	C_1	C_2	C_3	F_M
Pump	1.89	1.35	3.3892	0.0536	0.1538	-0.3935	0.3957	-0.00226	1.6
Turbine	-	-	2.7051	1.4398	-0.1776	-	-	-	6.2
Storage tank	2.25	1.82	3.4974	0.4485	0.1074	-	-	-	1.0

The cost values obtained from the literature were updated to 2019 using yearly values of the CEPCI (15, 119) using Eq. 5.34

$$C_j = C_i \left(\frac{I_j}{I_i}\right), \tag{5.34}$$

where the cost at year i, C_i, is updated to year j, C_j.

5.4 Methodology

The analysis was applied for the same fluids evaluated in chapter 4. This evaluation was divided in two parts in order to evaluate the performance of the proposed ORES system. In the first part, a quasi-steady state approach was applied to evaluate the system. Despite the transient nature of energy storage systems, it is a common practice to assume a quasi-steady state operation to allow for simpler algorithms and faster simulations (113). Under quasi-steady state operation there are two key parameters, namely pressure in the high pressure tank, P_{HPT}, and superheating degree at the turbine inlet ΔT_{SH}. In order to evaluate the effect of these parameters on system performance, η_{RT} was evaluated for ΔT_{SH} ranging from 0 up to 40 K, in steps of 5 K, and P_{HPT} ranging from 5% over the saturation pressure at ambient temperature up to 5% under the critical pressure.

In the second part, a transient analysis was applied to the system. The total volume at each tank are key parameters that affects both energy density and round-trip efficiency of the system. A Minimum Design Volume (which was designated here as "MDV") was defined for the LPT and HPT to standardize the analysis. The MDV for the HPT for a system with a discharge process with duration Δt_D was defined as the volume required such that the quality at the HPT would vary from 0.02 up to 0.98 and considering that the mass flow rate at $t = 0$, $\dot{m}_D^{t=0}$ would remain constant over the entire discharging process. The MDV for the LPT is similar but with a quality of 0.98 at the start and 0.02 at the end of the discharging process, as defined by Eqs. 5.35 and 5.36, respectively

$$MDV_{HPT} = \frac{\dot{m}_D^{t=0} \Delta t_D}{\rho_{HPT}^{t=0} - \rho_{HPT}^{t=t_{end}}}, \tag{5.35}$$

$$MDV_{LPT} = \frac{\dot{m}_D^{t=0} \Delta t_D}{\rho_{LPT}^{t=t_{end}} - \rho_{LPT}^{t=0}}, \tag{5.36}$$

where $\rho_{HPT}^{t=0}$ and $\rho_{HPT}^{t=t_{end}}$ are the specific mass of the HPT at the start and end of the process, respectively, and $\rho_{LPT}^{t=0}$ and $\rho_{LPT}^{t=t_{end}}$ the same for the LPT. The volumes of the HPT and LPT can then be set based on multiplication factors, K_{HPT} and K_{LPT} respectively, i.e. $V_{HPT} = K_{HPT}\ MDV_{HPT}$ and $V_{LPT} = K_{LPT}\ MDV_{LPT}$.

Initially, a transient analysis is performed for a single case, R-141b, with a starting pressure of $P_{HPT} = 3,200$ kPa and volume multiplication factors $K_{HPT} = 1$ and $K_{LPT} = 1$, to illustrate the transient conditions in the tanks and over the system. Then, the effect of the storage volume on η_{RT}, ρ_{E_V} and on the CAPEX was evaluated for K_{HPT} and K_{LPT} varying from 1.0 to 4.0, in steps of 0.125. In the transient analysis, the ORES system was evaluated considering operation of a medium-scale system ($\dot{W}_t = 1$ MW for 1h of operation). The Euler method was used for the solution of the set of differential equations in the transient analysis. Fig. 5.3 shows the flowchart of the algorithm used for the transient analysis.

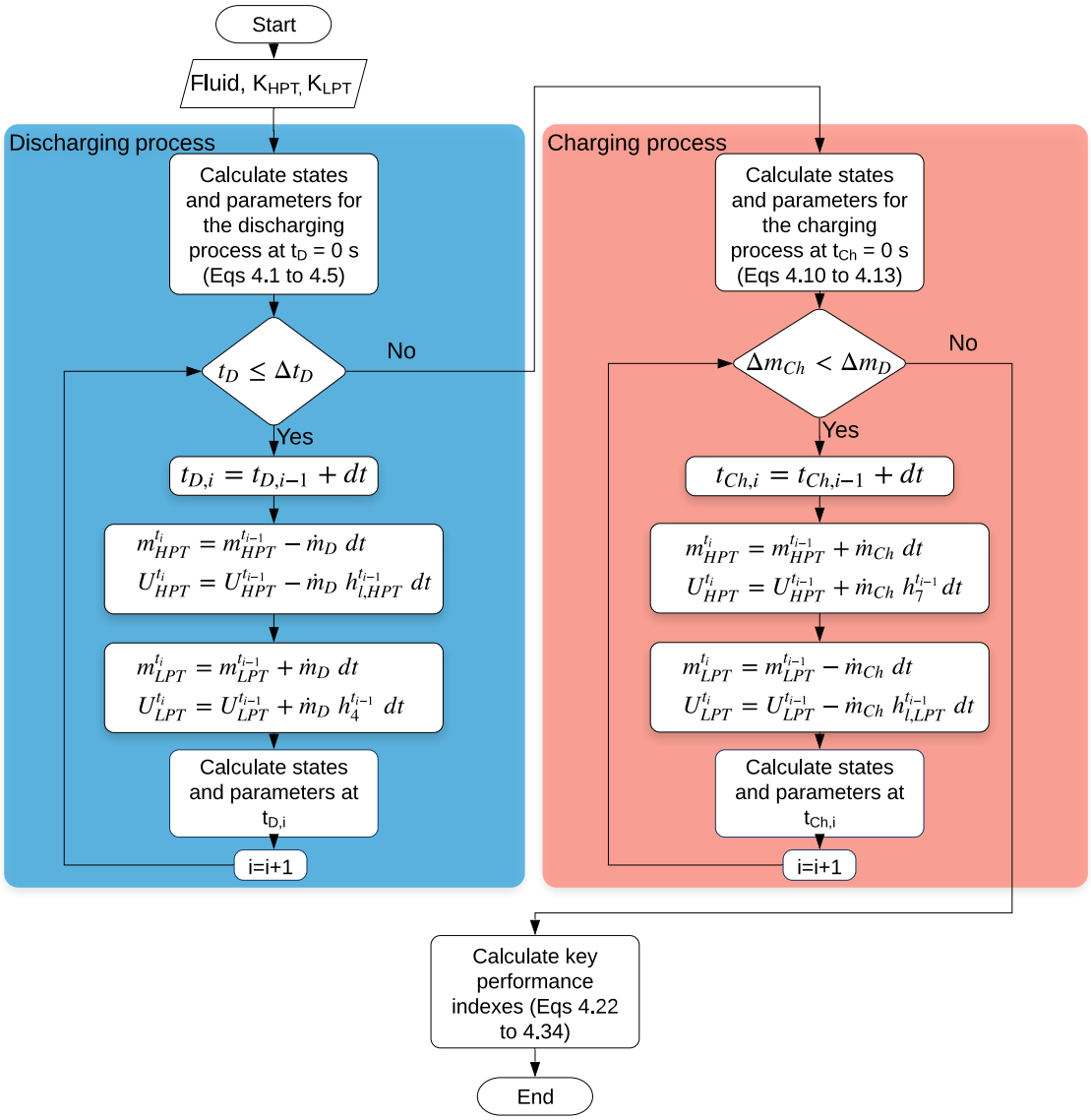

Figure 5.3 – Transient simulation algorithm flowchart.

Over the discharging/charging process there was a possibility of discontinuities in the equations of state, whenever this occurred the algorithm would assume a linear variation in the state at the tank, if this discontinuity would persist for over three points the simulation would be considered failed. The models of the system were implemented in MATLAB with the CoolProp external library for the thermodynamic properties (17). The assumptions and system parameters considered for these analysis are summarized on Table 5.2.

Table 5.2 – Assumptions and pre-defined parameters.

Ambient temperature, T_{amb}	25 °C
Ambient pressure, P_{amb}	101.3 kPa
Energy generation process duration, Δt_g	1 h
Turbine power, $\dot{W}_t$	1,000 kW
Pump power, $\dot{W}_p$	200 kW
Turbine isentropic efficiency, η_t	0.80 (34, 92)
Pump isentropic efficiency, η_p	0.75 (34, 92)
Isobaric heating and cooling	
Negligible pressure loss	

5.5 Results

5.5.1 Quasi-steady state analysis

The first part of the quasi-steady state analysis consisted in the evaluation of the round-trip efficiency as a function of P_{HPT} and ΔT_{SH} for each of the evaluated fluids. The results for the evaluated working fluids, in descending order of exergy density, are displayed in Figures 5.4a to 5.4e.

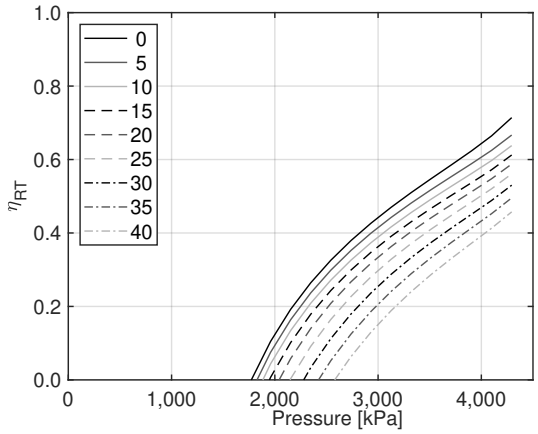

(a) R-152a

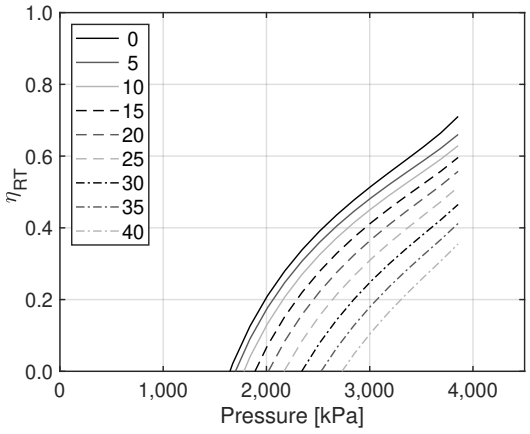

(b) R-134a

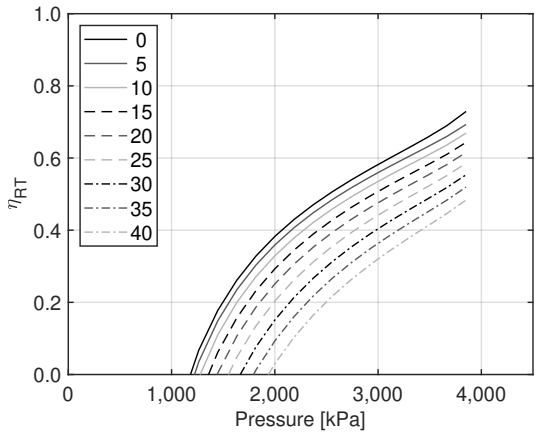

(c) R-142b

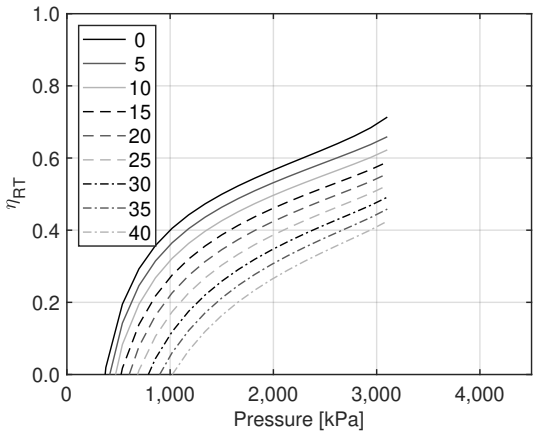

(d) R-365mfc

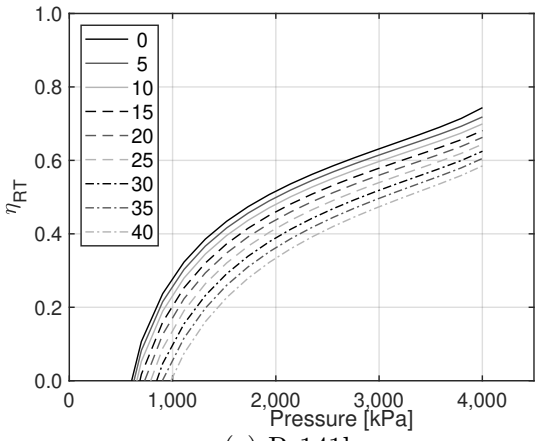

(e) R-141b

Figure 5.4 – Round-trip efficiency as a function of pressure at the high pressure tank, P_{HPT}, and superheating degree, ΔT_{SH}, for the evaluated organic fluids.

For all fluids a combination of high storage pressure and low superheating degree resulted in the highest values of round-trip efficiency. The maximum round-trip efficiency of the evaluated fluids ranged from 71%, for R-152a, up to 74%, for R-141b. For most fluids η_{RT} decreased linearly with the increase of the superheating degree, except for R-152a, that showed increased gradients for higher superheating degrees. In general, an increment of 5 K in the superheating degree resulted in an absolute 3-5% reduction in the round-trip efficiency, except for R-141b, which showed a reduction of 2% for each increment. Regarding pressure, an average reduction of 10% in η_{RT} for each reduction of 500 kPa in P_{HPT} was observed for the higher values of efficiency for R-152a, R-134a and R-142b. On the other hand, R-365mfc and R-141b were much less affected by the variation in pressure, which translates into a wider range of pressures with a positive round-trip efficiency. This suggests that, over the discharging and charging phase of the energy storage system, as pressure in both tanks change due to the transient states inherent to both processes, the performance of the system is more stable while also allowing for a higher discharge of the storage tank, that can now discharge to lower pressures. Figure 5.5 displays the results for all fluids in a single graph.

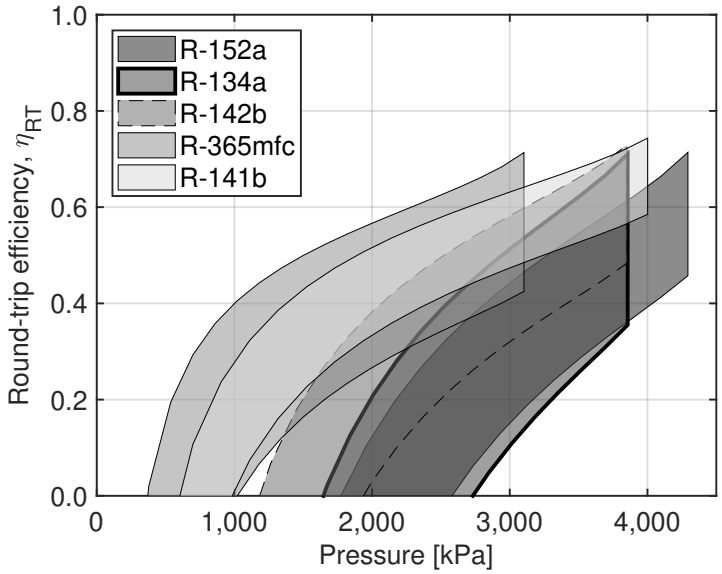

Figure 5.5 – Comparison of round-trip efficiency as a function of P_{HPT} and ΔT_{SH} for the evaluated organic fluids.

Figure 5.5 shows more clearly the difference in performance among working fluids. All fluids achieve efficiencies over 70%. R-365mfc and R-141b showed clear dominance over the remaining working fluids over the range of evaluated pressures with R-365mfc having higher η_{RT} over the range of P_{HPT} from 500 kPa up to 3,100 kPa and R-141b from 3,250 up to 4,000 kPa. It should be noted that R-141b also maintains a round-trip efficiency over 50% for a wide range of pressure values, from 1.9 MPa up to 4.0 MPa, suggesting good transient performance.

5.5.2 Transient analysis

The results of the quasi-steady state analysis provide reasonable reference values in terms of efficiency, but a transient analysis is required to understand how the parameters of the system change over a full cycle, allowing the calculation of the energy density. First, a transient simulation for an ORES system operating with R-141b and P_{HPT} of 3,200 kPa was carried out. The variation of the properties over the charging and discharging processes is displayed in Fig. 5.6.

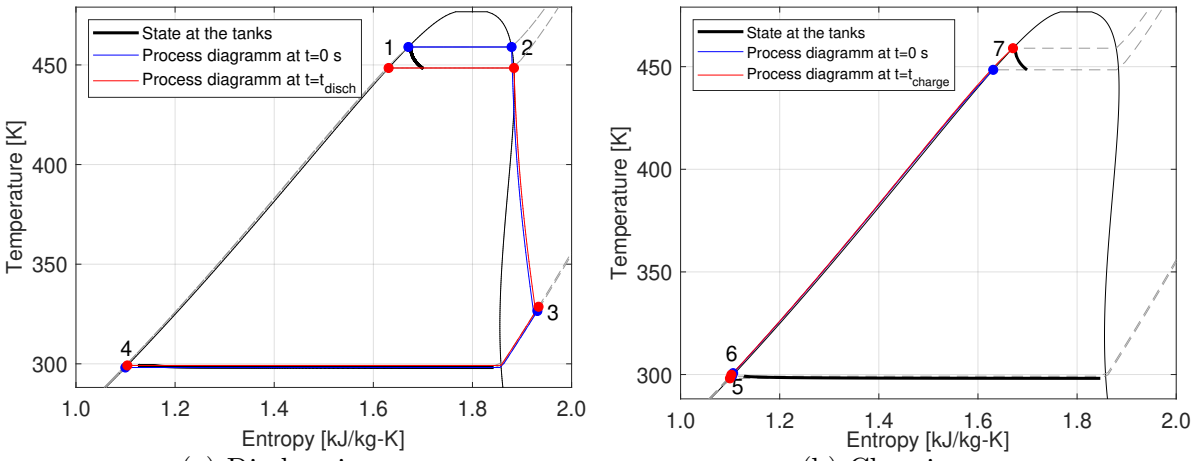

(a) Discharging process (b) Charging process

Figure 5.6 – T-s diagrams for the start and end states of the discharging and charging processes for a transient simulation of an ORES system.

This particular case resulted in a round-trip efficiency of 62%, compared to 65% for the quasi-steady state analysis, and an energy density of 1.15 kWh m^{-3}. Pressure at the HPT is the variable with the highest variation over the process, dropping from 3,200 kPa at the start of the discharging process down to 2,400 kPa, whilst the temperature drops from 460 K down to 440 K.

To better understand the role of the storage vessels, the transient analysis was expanded to all of the evaluated working fluids varying the volume multiplication factor for both the high and low pressure tanks, K_{HPT} and K_{LPT}. The round-trip efficiency, energy density and CAPEX for K_{HPT} and K_{LPT} ranging from 1.0 up to 4.0 were then calculated and the results are displayed in Figs 5.7 and 5.8.

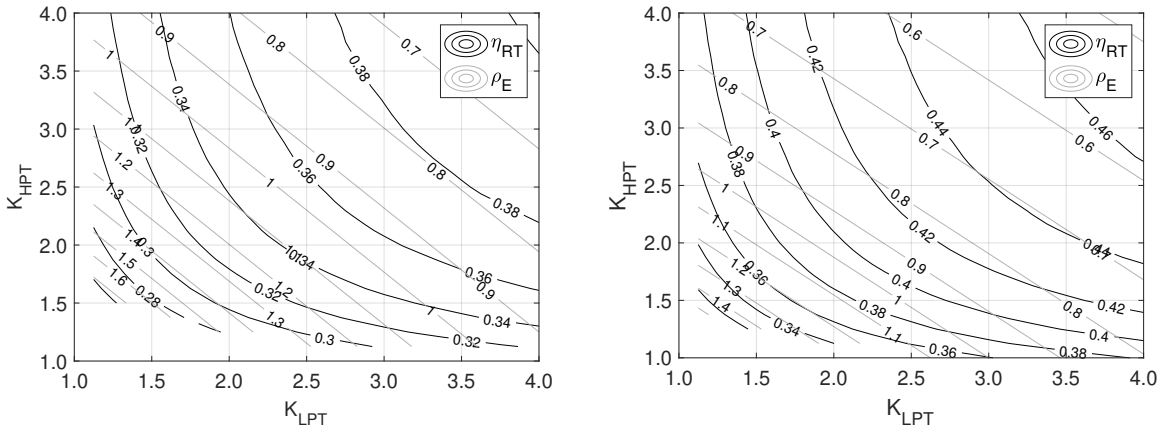

(a) R-152a (b) R-134a

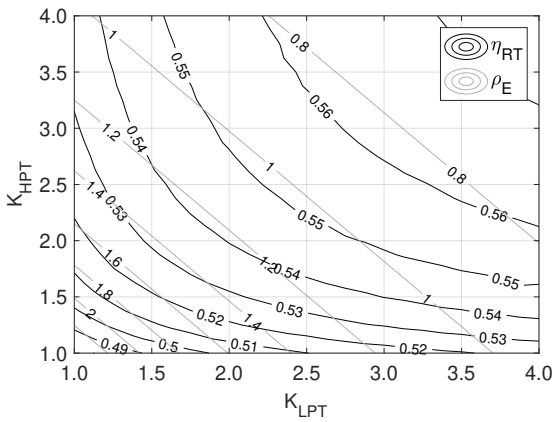

(c) R-142b

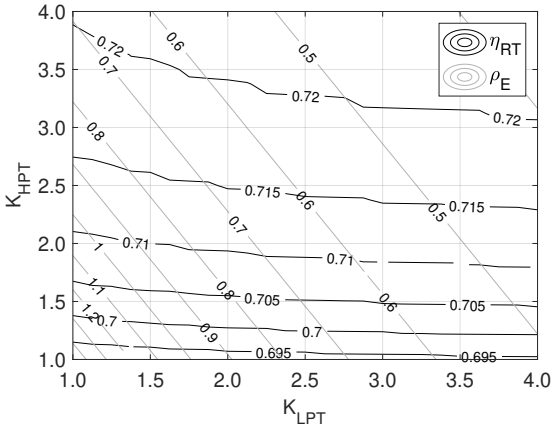

(d) R-365mfc

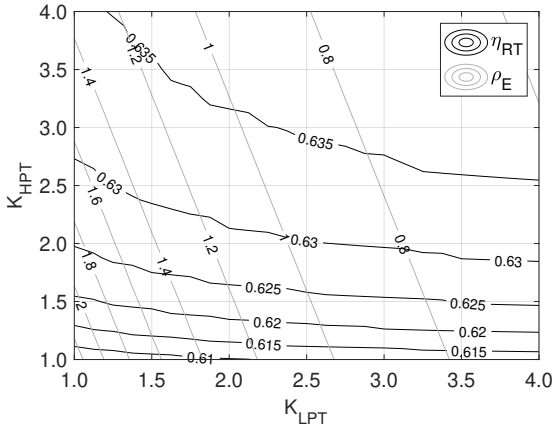

(e) R-141b

Figure 5.7 – Round-trip efficiency, η_{RT}, and energy density, ρ_E in kWh m^{-3}, as a function of high and low pressure tank volume multiplication factors, K_{HPT} and K_{LPT}, respectively.

The obtained round-trip efficiencies are comparable to those reported for CAES and LAES (25-75 %) (63, 120, 121). Relative to the influence of volume on performance parameters it can be seen that the volume of the LPT showed smaller effect on η_{RT}, in special for systems with $K_{HPT} < 2$ and for the working fluids that showed higher round-trip efficiency. As a higher volume was used, the overall variation in the operation parameters is reduced, which results in the operation at higher round-trip efficiency conditions while reducing the energy density. Both volumes contributed similarly to energy density, except for R-141b, for which the LPT had approximately doubled the impact on the energy density.

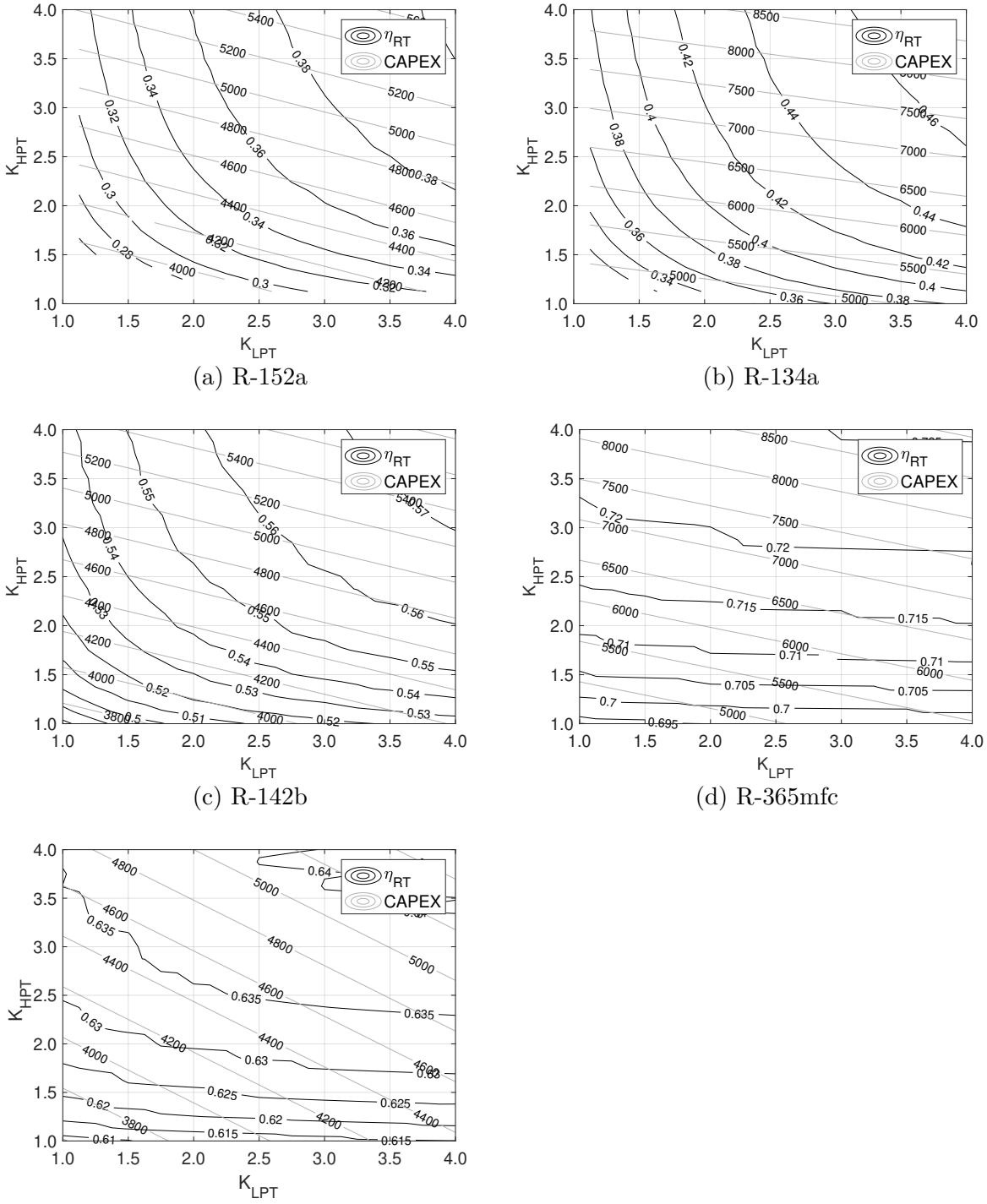

(a) R-152a

(b) R-134a

(c) R-142b

(d) R-365mfc

(e) R-141b

Figure 5.8 – Round-trip efficiency, η_{RT}, and CAPEX (USD per kWh) as a function of high and low pressure tank volume multiplication factors, K_{HPT} and K_{LPT}, respectively.

The CAPEX of all fluids, except R-141b, was greatly influenced by the volume of the HPT, indicating the predominance of the cost of the high pressure vessel over the overall cost of the system, with R-134a and R-365mfc presenting the highest CAPEX. For a better comparison, results obtained previously for all fluids are summarized in Fig. 5.9. The maximum (black markers) and minimum (gray markers) values of η_{RT} and

CAPEX are pointed, therefore defining the region that contains all points calculated for the respective fluid.

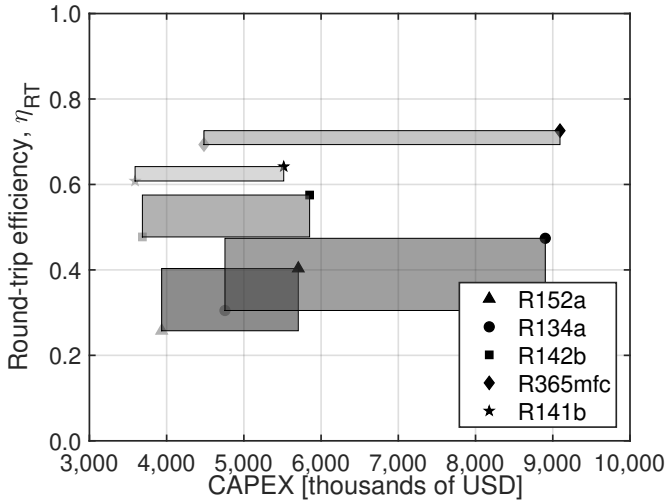

Figure 5.9 – Comparison of range of values of η_{RT} and CAPEX (maximum in black and minimum in grey) for each of the evaluated working fluids.

The difference between maximum and minimum η_{RT} was relatively small, under 5%, for the working fluids with higher efficiency (R-365mfc and R-141b) and around double this value for the remaining fluids. R-365mfc had higher round-trip efficiencies (ranging from 69 to 73%) for all the studied parameters with a wide variation of CAPEX, while R-141b had the second highest efficiency (61 to 64%), but concentrated on lower CAPEX. As the order of magnitude of turbine, pump and auxiliary components costs are similar compared to CAES, ORES can be even cheaper than above ground CAES, depending on the costs of the Thermal Energy Storage.

5.6 Conclusions

This chapter evaluated the potential application of the ORES system, based on a thermodynamic and cost analysis, as an alternative to CAES and LAES. The system was studied considering operation with five organic fluids, pre-selected on chapter 4. Initially, the effects of pressure and superheating degree on round-trip efficiency based on a quasi-steady state model was studied. Then, the system was evaluated based on a transient analysis.

The round-trip efficiency for the quasi-steady state analysis reached over 70% for all fluids, with R-141b having the highest efficiency, 74%, comparable to analytical results for CAES and LAES with similar considerations. An increase in the superheating degree resulted in a reduction of 3-5% in round-trip efficiency for an increment of 5 K for most fluids. Pressure had a contrary effect, an increase in pressure promoted an increment in efficiency, with a reasonable range of pressure values for which round-trip efficiency was

higher than 50%. The efficiency was over 50% for a reasonable range of pressures for all fluids, with difference between pressure at maximum efficiency and at efficiency equal to 50% ranging from 1,000 kPa for R-134a up to 2,000 kPa for R-141b. The importance of this range is that it indicates the stability in system efficiency as the pressure varies during a transient process. R-141b showed smaller sensitivity regarding both, superheating degree and pressure, relative to the other organic fluids indicating it may present higher efficiencies in off-design conditions.

The system was then studied considering transient conditions in terms of round-trip efficiency, energy density and CAPEX. First, the transient analysis model was used to study the variation of the properties of the system over an operation cycle for R-141b. A round-trip efficiency of 62% was obtained, compared to 65% for the same case analyzed under quasi-steady state conditions. Pressure dropped from 3,200 kPa down to 2,400 kPa whilst temperature dropped from 460 K down to 440 K. Then, the operation of the ORES system was evaluated for all five organic fluids for K_{HPT} and K_{LPT} ranging from 1.0 to 4.0. The higher the volume of the tanks the lower the energy density while round-trip efficiency is higher because there is a smaller variation in system parameters. Energy density ranged from 0.5 up to 2.2 kWh m^{-3}, even lower than CAES. The current topology for the ORES system resulted in competitive cost and efficiency but did not achieve the potential energy density expected from the previous chapter.

6 Conclusions and proposals of future research

6.1 Conclusions

This work evaluated the use of organic fluids as an energy storage medium with focus on the application to long-term energy storage. First, the potential of organic fluids for energy storage was evaluated in Chapter 4 in terms of the maximum energy density possible, in the form of the exergy density, and the CAPEX of the storage tank. The analysis was applied to five organic fluids (R-152a, R-134a, R-142b, R-365mfc and R-141b) that were selected based on commercial maturity, safety classification and environmental impact, namely ODP and GWP.

The exergy density and CAPEX of the storage tank were evaluated for storage pressures ranging from 5% over the saturation pressure at ambient temperature up to 5% lower than the critical pressure and compared to compressed air, with storage pressure from ambient pressure up to 8,000 kPa, and liquid air at ambient pressure and temperature of 78 K. The exergy density, in terms of volume, for all fluids was higher than those calculated for compressed air, even for compressed at double the storage pressure (achieving 8 up 15 kWh m^{-3}, depending on the fluid while compressed air maximum exergy density reaches 6 kWh m^{-3}), but still reasonably smaller than the exergy density for liquid air, with 180 kWh m^{-3}.

Then, the CAPEX of the storage system (storage tank and fluid) was evaluated for the organic fluids and for compressed air. The cost of the tank itself is lower for organic fluids, as their operational pressure is much lower than that for compressed air, but the working fluid must also be included, which, for the case of CAES, is free. The cost of the storage system, for the same storage volume, was of the same order of magnitude as compressed air for R-134a, R-142b, R-365mfc and R-141b. However, because of the higher exergy density of the organic fluids, they have a higher energy storage capacity and, consequently, their cost per unit of stored energy is lower than that of compressed air. The minimum cost per unit energy for the remaining working fluids were 1,526 \$ kWh^{-1} for R-141b, 2,090 \$ kWh^{-1} for R-134a, 2,162 \$ kWh^{-1} for R-142b and 2,388 \$ kWh^{-1} for R-365mfc while the minimum cost for compressed air was of 2,769 \$ kWh^{-1}, i.e. from 16% to 80% higher than for the organic fluids.

The results from Chapter 4 indicate that the organic fluids as an energy storage medium can store energy with a higher energy density than compressed air and at a lower cost per unit energy. This is mainly related to the reduction in cost due to the operation

at lower pressures would also affect the cost of the other equipments of energy system, such as heat exchangers, piping and pump.

In Chapter 5 an energy storage system based on the Organic Rankine Cycle was proposed and was evaluated in terms of round-trip efficiency, energy density and CAPEX and the influence of pressure, superheating degree, high and low pressure storage volume in these performance indexes. The analysis was divided in two parts, in the first the system was evaluated based on a quasi-steady state analysis while in the second the system was evaluated based on a transient analysis. During both quasi-steady state and transient analysis the system achieved efficiencies competitive to CAES and LAES systems, with the maximum round-trip efficiency for the system with R-365mfc, 73%, but with low energy density, even lower than for CAES systems. The present results indicate that the ORES system has the potential to be an alternative to CAES and LAES as a medium-scale, long-duration energy storage system but some work must be invested in further improving its energy density.

6.2 Proposals of future research

The theoretical potential of the ORES system observed in this study indicates that the sizing and construction of a prototype system is the most indicated next step in this research. As this is only the first study on energy storage with organic fluids as the storage medium it is believed that there is a high potential of improvement for the system. Considering the properties discussed in Chapter 3, the following research topics are suggested:

- Experimental validation of the results of this study;
- Expansion of the study to other organic fluids;
- Evaluation of organic fluid mixtures, varying mixture components and composition;
- Evaluation of supercritical cycles;
- Incorporation of thermal energy storage to improve cycle efficiency;
- Implementation of operational maps for evaluation of off-design operation conditions and technology constraints; and
- Proposal and evaluation of new topologies for energy storage, such as the use of recuperators and multi-stage expansion.

Bibliography

1 ONS. *Histórico da Operação*. Brazil: ONS, 2020. http://www.ons.org.br/Paginas/resultados-da-operacao/historico-da-operacao/curva_carga_horaria.aspx. Accessed: 2020-03-06.

2 GREENWOOD, D. et al. Frequency response services designed for energy storage. *Applied Energy*, v. 203, p. 115–127, 2017.

3 TAN, X.; LI, Q.; WANG, H. Advances and trends of energy storage technology in Microgrid. *International Journal of Electrical Power & Energy Systems*, v. 44, n. 1, p. 179–191, 2013.

4 ANEKE, M.; WANG, M. Energy storage technologies and real life applications – A state of the art review. *Applied Energy*, v. 179, p. 350–377, 2016.

5 STEINMANN, W.-D. Thermo-mechanical concepts for bulk energy storage. *Renewable and Sustainable Energy Reviews*, v. 75, p. 205–219, 2017.

6 SATKIN, M. et al. Multi criteria site selection model for wind-compressed air energy storage power plants in Iran. *Renewable and Sustainable Energy Reviews*, v. 32, p. 579–590, 2014.

7 CHEN, J. et al. Preliminary investigation on the feasibility of a clean caes system coupled with wind and solar energy in china. *Energy*, v. 127, p. 462–478, 2017.

8 ZHANG, Y. et al. Thermodynamic analysis of a novel energy storage system with carbon dioxide as working fluid. *Renewable Energy*, v. 99, p. 682–697, 2016.

9 QUOILIN, S. et al. Thermo-economic survey of Organic Rankine Cycle (ORC) systems. *Renewable and Sustainable Energy Reviews*, v. 22, p. 168–186, 2013.

10 XU, H.; GAO, N.; ZHU, T. Investigation on the fluid selection and evaporation parametric optimization for sub- and supercritical organic Rankine cycle. *Energy*, v. 96, p. 59–68, 2016.

11 BAHADORMANESH, N.; RAHAT, S.; YARALI, M. Constrained multi-objective optimization of radial expanders in organic Rankine cycles by firefly algorithm. *Energy Conversion and Management*, v. 148, p. 1179–1193, 2017.

12 ASHRAE. *ASHRAE Standard 15 & 34*. [S.l.]: ASHRAE, 2020. https://www.ashrae.org/technical-resources/bookstore/standards-15-34. Accessed: 2020-03-11.

13 RAHBAR, K. et al. Review of organic Rankine cycle for small-scale applications. *Energy Conversion and Management*, v. 134, p. 135–155, 2017.

14 MACCHI, E.; ASTOLFI, M. *Organic Rankine Cycle (ORC) Power Systems Technologies and Applications*. [S.l.]: Woodhead Publishing, 2017.

15 TURTON, R. et al. *Analysis, Synthesis, and Design of Chemical Processes*. 5th edition. ed. [S.l.]: Pearson Education, Inc., 2018.

16 KAZEMI, N.; SAMADI, F. Thermodynamic, economic and thermo-economic optimization of a new proposed organic Rankine cycle for energy production from geothermal resources. *Energy Conversion and Management*, v. 121, p. 391–401, 2016.

17 BELL, I. H. et al. Pure and pseudo-pure fluid thermophysical property evaluation and the open-source thermophysical property library coolprop. *Industrial & Engineering Chemistry Research*, v. 53, n. 6, p. 2498–2508, 2014.

18 LE, V. L. et al. Thermodynamic and economic optimizations of a waste heat to power plant driven by a subcritical ORC (Organic Rankine Cycle) using pure or zeotropic working fluid. *Energy*, v. 78, p. 622–638, 2014.

19 PEZZUOLO, A. et al. The ORC-PD: A versatile tool for fluid selection and Organic Rankine Cycle unit design. *Energy*, v. 102, p. 605–620, 2016.

20 IRENA. *Global Energy Transformation: A roadmap to 2050*. Abu Dhabi, 2018.

21 LUO, X. et al. Overview of current development in electrical energy storage technologies and the application potential in power system operation. *Applied Energy*, v. 137, p. 511–536, 2015.

22 BOCKLISCH, T. Hybrid Energy Storage Systems for Renewable Energy Applications. *Energy Procedia*, v. 73, p. 103–111, 2015.

23 HEMMATI, R.; SABOORI, H. Emergence of hybrid energy storage systems in renewable energy and transport applications – A review. *Renewable and Sustainable Energy Reviews*, v. 65, p. 11–23, 2016.

24 KYRIAKOPOULOS, G. L.; ARABATZIS, G. Electrical energy storage systems in electricity generation: Energy policies, innovative technologies, and regulatory regimes. *Renewable and Sustainable Energy Reviews*, v. 56, p. 1044–1067, 2016.

25 ARGYROU, M. C.; CHRISTODOULIDES, P.; KALOGIROU, S. A. Energy storage for electricity generation and related processes: Technologies appraisal and grid scale applications. *Renewable and Sustainable Energy Reviews*, v. 94, p. 804–821, 2018.

26 EVANS, A.; STREZOV, V.; EVANS, T. Assessment of utility energy storage options for increased renewable energy penetration. *Renewable and Sustainable Energy Reviews*, v. 16, p. 4141–4147, 2012.

27 CHATZIVASILEIADI, A.; AMPATZI, E.; KNIGHT, I. Characteristics of electrical energy storage technologies and their applications in buildings. *Renewable and Sustainable Energy Reviews*, v. 25, p. 814–830, 2013.

28 AKINYELE, D.; RAYUDU, R. Review of energy storage technologies for sustainable power networks. *Sustainable Energy Technologies and Assessments*, v. 8, p. 74–91, 2014.

29 SCIACOVELLI, A.; VECCHI, A.; DING, Y. Liquid air energy storage (LAES) with packed bed cold thermal storage - From component to system level performance through dynamic modelling. *Applied Energy*, v. 190, p. 84–98, 2017.

30 PORTO, M. et al. An alternative solution based on compressed and liquefied air storage systems for reducing power output variability from PV solar farms. In: *Proceedings of the 22nd International Congress of Mechanical Engineering*. [S.l.: s.n.], 2013. p. 1005–1014.

31 KANTHARAJ, B.; GARVEY, S.; PIMM, A. Compressed air energy storage with liquid air capacity extension. *Applied Energy*, v. 157, p. 152–164, 2015.

32 SMALLBONE, A. et al. Levelised Cost of Storage for Pumped Heat Energy Storage in comparison with other energy storage technologies. *Energy Conversion and Management*, v. 152, p. 221–228, 2017.

33 DESAI, N. B.; BANDYOPADHYAY, S. Thermo-economic analysis and selection of working fluid for solar organic Rankine cycle. *Applied Thermal Engineering*, v. 95, p. 471–481, 2016.

34 LECOMPTE, S. et al. Review of Organic Rankine cycle (ORC) architectures for waste heat recovery. *Renewable and Sustainable Energy Reviews*, v. 47, p. 448–461, 2015.

35 LI, J. et al. Effect of working fluids on the performance of a novel direct vapor generation solar organic Rankine cycle system. *Applied Thermal Engineering*, v. 98, p. 786–797, 2016.

36 SUNG, T.; KIM, K. C. Thermodynamic analysis of a novel dual-loop organic rankine cycle for engine waste heat and LNG cold. *Applied Thermal Engineering*, v. 100, p. 1031–1041, 2016.

37 UUSITALO, A. et al. Experimental study on charge air heat utilization of large-scale reciprocating engines by means of Organic Rankine Cycle. *Applied Thermal Engineering*, v. 89, p. 209–219, 2015.

38 PERIS, B. et al. Experimental study of an ORC (organic Rankine cycle) for low grade waste heat recovery in a ceramic industry. *Energy*, v. 85, p. 534–542, 2015.

39 XI, H. et al. A graphical criterion for working fluid selection and thermodynamic system comparison in waste heat recovery. *Applied Thermal Engineering*, v. 89, p. 772–782, 2015.

40 BRAIMAKIS, K. et al. Low grade waste heat recovery with subcritical and supercritical Organic Rankine Cycle based on natural refrigerants and their binary mixtures. *Energy*, v. 88, p. 80–92, 2015.

41 JRADI, M.; RIFFAT, S. Experimental investigation of a biomass-fuelled micro-scale tri-generation system with an organic Rankine cycle and liquid desiccant cooling unit. *Energy*, v. 71, p. 80–93, 2014.

42 URIS, M.; LINARES, J. I.; ARENAS, E. Size optimization of a biomass-fired cogeneration plant CHP/CCHP (Combined heat and power/Combined heat, cooling and power) based on Organic Rankine Cycle for a district network in Spain. *Energy*, v. 88, p. 935–945, 2015.

43 IMRAN, M. et al. Comparative assessment of Organic Rankine Cycle integration for low temperature geothermal heat source applications. *Energy*, v. 102, p. 473–490, 2016.

44 MOKHTARI, H. et al. Determination of optimum geothermal Rankine cycle parameters utilizing coaxial heat exchanger. *Energy*, v. 102, p. 260–275, 2016.

45 CEBULLA, F. et al. How much electrical energy storage do we need? A synthesis for the U.S., Europe, and Germany. *Journal of Cleaner Production*, v. 181, p. 449–459, 2018.

46 BLANCO, H.; FAAIJ, A. A review at the role of storage in energy systems with a focus on Power to Gas and long-term storage. *Renewable and Sustainable Energy Reviews*, v. 81, p. 1049–1086, 2018.

47 LEONARD, M. D.; MICHAELIDES, E. E.; MICHAELIDES, D. N. Energy storage needs for the substitution of fossil fuel power plants with renewables. *Renewable Energy*, v. 145, p. 951–962, 2020.

48 LI, Y. *Cryogen Based Energy Storage: Process Modelling and Optimisation*. Tese (Doutorado) — University of Birmingham, 2011.

49 GÜNTER, N.; MARINOPOULOS, A. Energy storage for grid services and applications: Classification, market review, metrics, and methodology for evaluation of deployment cases. *Journal of Energy Storage*, v. 8, p. 226–234, 2016.

50 SABIHUDDIN, S. et al. A Numerical and Graphical Review of Energy Storage Technologies. *Energies*, v. 8, n. 1, p. 172–216, 2014.

51 CHEN, H. et al. Progress in electrical energy storage system: A critical review. *Progress in Natural Science*, v. 19, n. 3, p. 291–312, 2009.

52 FERREIRA, H. L. et al. Characterisation of electrical energy storage technologies. *Energy*, v. 53, p. 288–298, 2013.

53 SUCCAR, S.; WILLIAMS, R. H. *Compressed Air Energy Storage: Theory, Resources, And Applications For Wind Power*. Princeton Environmental Institute, 2008.

54 BERRADA, A.; LOUDIYI, K.; ZORKANI, I. Profitability, risk, and financial modeling of energy storage in residential and large scale applications. *Energy*, v. 119, p. 94–109, 2017.

55 ROUINDEJ, K.; SAMADANI, E.; FRASER, R. A. CAES by design: A user-centered approach to designing Compressed Air Energy Storage (CAES) systems for future electrical grid: A case study for Ontario. *Sustainable Energy Technologies and Assessments*, v. 35, p. 58–72, 2019.

56 SADREDDINI, A. et al. Exergy analysis and optimization of a CCHP system composed of compressed air energy storage system and ORC cycle. *Energy Conversion and Management*, v. 157, p. 111–122, 2018.

57 CHEAYB, M. et al. Modelling and experimental validation of a small-scale trigenerative compressed air energy storage system. *Applied Energy*, v. 239, p. 1371–1384, 2019.

58 VENKATARAMANI, G. et al. Thermodynamic analysis on compressed air energy storage augmenting power / polygeneration for roundtrip efficiency enhancement. *Energy*, v. 180, p. 107–120, 2019.

59 HAHN, H. et al. Techno-economic assessment of a subsea energy storage technology for power balancing services. *Energy*, v. 133, p. 121–127, 2017.

60 BARNES, F. S.; LEVINE, J. G. *Large Energy Storage Systems Handbook*. 1st. ed. Boca Raton, FL: CRC Press, 2011.

61 HAMDY, S.; MOROSUK, T.; TSATSARONIS, G. Cryogenics-based energy storage: Evaluation of cold exergy recovery cycles. *Energy*, v. 138, p. 1069–1080, 2017.

62 DING, Y. et al. Cryogenic Energy Storage. In: *Handbook of Clean Energy Systems*. [S.l.]: John Wiley & Sons, Ltd, 2015. p. 1–15.

63 PENG, X. et al. Thermodynamic study on the effect of cold and heat recovery on performance of liquid air energy storage. *Applied Energy*, v. 221, p. 86–99, 2018.

64 XIE, C. et al. An economic feasibility assessment of decoupled energy storage in the UK: With liquid air energy storage as a case study. *Applied Energy*, v. 225, p. 244–257, 2018.

65 DAMAK, C. et al. Liquid Air Energy Storage (LAES) as a large-scale storage technology for renewable energy integration - A review of investigation studies and near perspectives of LAES. *International Journal of Refrigeration*, v. 110, p. 208–218, 2020.

66 LEGRAND, M. et al. Integration of liquid air energy storage into the spanish power grid. *Energy*, v. 187, p. 115965, 2019.

67 VECCHI, A. et al. Integrated techno-economic assessment of Liquid Air Energy Storage (LAES) under off-design conditions: Links between provision of market services and thermodynamic performance. *Applied Energy*, v. 262, p. 114589, 2020.

68 LIU, H. et al. Thermodynamic analysis of a compressed carbon dioxide energy storage system using two saline aquifers at different depths as storage reservoirs. *Energy Conversion and Management*, v. 127, p. 149–159, 2016.

69 WANG, G.-B.; ZHANG, X.-R. Thermodynamic analysis of a novel pumped thermal energy storage system utilizing ambient thermal energy and LNG cold energy. *Energy Conversion and Management*, v. 148, p. 1248–1264, 2017.

70 HE, Q. et al. Thermodynamic analysis of a novel supercritical compressed carbon dioxide energy storage system through advanced exergy analysis. *Renewable Energy*, v. 127, p. 835–849, 2018.

71 FRATE, G. F.; ANTONELLI, M.; DESIDERI, U. A novel Pumped Thermal Electricity Storage (PTES) system with thermal integration. *Applied Thermal Engineering*, v. 121, p. 1051–1058, 2017.

72 ROSKOSCH, D.; ATAKAN, B. Pumped Heat Electricity Storage: Potential Analysis and ORC Requirements. *Energy Procedia IV International Seminar on ORC Power Systems*, v. 129, p. 1026–1033, 2017.

73 GUO, J. et al. Performance characteristics and parametric optimizations of a weak dissipative pumped thermal electricity storage system. *Energy Conversion and Management*, v. 157, p. 527–535, 2018.

74 HAJIAGHASI, S.; SALEMNIA, A.; HAMZEH, M. Hybrid energy storage system for microgrids applications: A review. *Journal of Energy Storage*, v. 21, p. 543–570, 2019.

75 COLONNA, P. et al. Organic Rankine Cycle Power Systems: From the Concept to Current Technology, Applications, and an Outlook to the Future. *Journal of Engineering for Gas Turbines and Power*, v. 137, n. 10, p. 1–19, 2015.

76 MAHMOUDI, A.; FAZLI, M.; MORAD, M. A recent review of waste heat recovery by Organic Rankine Cycle. *Applied Thermal Engineering*, v. 143, p. 660–675, 2018.

77 ASHRAE. *ANSI/ASHRAE Standard 34-2016 - Designation and Safety Classification of Refrigerants - addendum g*. Atlanta, GA, 2018.

78 OZONE Depleting Substances. [S.l.]: United States Environmental Protection Agency, 2020. https://www.epa.gov/ozone-layer-protection/ozone-depleting-substances#self. Accessed: 2020-03-11.

79 UNDERSTANDING global warming potentials. [S.l.]: United States Environmental Protection Agency, 2020. https://www.epa.gov/ghgemissions/understanding-global-warming-potentials. Accessed: 2020-03-11.

80 SONG, P. et al. A review of scroll expanders for organic Rankine cycle systems. *Applied Thermal Engineering*, v. 75, p. 54–64, 2015.

81 RICHTER, L. Screw engine used as an expander in ORC for low-potential heat utilization Experimental investigation of a supersonic micro turbine running with hexamethyldisiloxane. *AIP Conference Proceedings*, v. 101, p. 20032–20050, 2017.

82 PETHURAJAN, V.; SIVAN, S.; JOY, G. C. Issues, comparisons, turbine selections and applications – An overview in organic Rankine cycle. *Energy Conversion and Management*, v. 166, p. 474–488, 2018.

83 LECOMPTE, S. et al. Multi-Objective Thermo-Economic Optimization Strategy for ORCs Applied to Subcritical and Transcritical Cycles for Waste Heat Recovery. *Energies*, v. 8, n. 4, p. 2714–2741, 2015.

84 GUO, C. et al. Performance analysis of organic Rankine cycle based on location of heat transfer pinch point in evaporator. *Applied Thermal Engineering*, v. 62, n. 1, p. 176–186, 2014.

85 PAN, L.; WANG, H.; SHI, W. Performance analysis in near-critical conditions of organic Rankine cycle. *Energy*, v. 37, n. 1, p. 281–286, 2012.

86 LARSEN, U. et al. Design and optimisation of organic Rankine cycles for waste heat recovery in marine applications using the principles of natural selection. *Energy*, v. 55, p. 803–812, 2013.

87 ANDREASEN, J. et al. Selection and optimization of pure and mixed working fluids for low grade heat utilization using organic Rankine cycles. *Energy*, v. 73, p. 204–213, 2014.

88 MAVROU, P. et al. Selection of working fluid mixtures for flexible Organic Rankine Cycles under operating variability through a systematic nonlinear sensitivity analysis approach. *Applied Thermal Engineering*, v. 89, p. 1054–1067, 2015.

89 ABADI, G. B.; YUN, E.; KIM, K. C. Experimental study of a 1kw organic Rankine cycle with a zeotropic mixture of R245fa/R134a. *Energy*, v. 93, p. 2363–2373, 2015.

90 LI, G. Organic Rankine cycle performance evaluation and thermoeconomic assessment with various applications part II: Economic assessment aspect. *Renewable and Sustainable Energy Reviews*, v. 64, p. 490–505, 2016.

91 SU, W.; ZHAO, L.; DENG, S. Simultaneous working fluids design and cycle optimization for organic rankine cycle using group contribution model. *Applied Energy*, v. 202, p. 618–627, 2017.

92 HÆRVIG, J.; SØRENSEN, K.; CONDRA, T. Guidelines for optimal selection of working fluid for an organic Rankine cycle in relation to waste heat recovery. *Energy*, v. 96, p. 592–602, 2016.

93 LINKE, P.; PAPADOPOULOS, A.; SEFERLIS, P. Systematic Methods for Working Fluid Selection and the Design, Integration and Control of Organic Rankine Cycles - A review. *Energies*, v. 8, p. 4755–4801, 2015.

94 SEYEDKAVOOSI, S.; JAVAN, S.; KOTA, K. Exergy-based optimization of an organic rankine cycle (orc) for waste heat recovery from an internal combustion engine (ice). *Applied Thermal Engineering*, v. 126, n. 5, p. 447–457, 2017.

95 FANG, Y.; YANG, F.; ZHANG, H. Comparative analysis and multi-objective optimization of organic Rankine cycle (ORC) using pure working fluids and their zeotropic mixtures for diesel engine waste heat recovery. *Applied Thermal Engineering*, v. 157, p. 113704, 2019.

96 MARAVER, D. et al. Systematic optimization of subcritical and transcritical organic Rankine cycles (ORCs) constrained by technical parameters in multiple applications. *Applied Energy*, v. 117, p. 11–29, 2014.

97 ASTOLFI, M. Techno-economic Optimization of Low Temperature CSP Systems Based on ORC with Screw Expanders. *Energy Procedia*, v. 69, p. 1100–1112, 2015.

98 LUO, X. et al. Thermo-economic analysis and optimization of a zoetropic fluid organic Rankine cycle with liquid-vapor separation during condensation. *Energy Conversion and Management*, v. 148, p. 517–532, 2017.

99 WU, Q. et al. Design and operation optimization of organic Rankine cycle coupled trigeneration systems. *Energy*, Pergamon, v. 142, p. 666–677, 2018.

100 ÇENGEL, Y. A.; BOLES, M. A. *Termodinâmica*. 7th. ed. New York, New York: McGraw-Hill Companies Inc., 2013.

101 MOSS, D. R.; BASIC, M. *Pressure Vessel Design Manual*. Fourth. Oxford: Elsevier, 2013.

102 LOZOWSKI, D. *The Chemical Engineering Plant Cost Index*. [S.l.]: Chemical Engineering, 2020. https://www.chemengonline.com/pci-home. Accessed: 2020-03-23.

103 BAO, J.; ZHAO, L. A review of working fluid and expander selection for organic Rankine cycle. *Renewable and Sustainable Energy Reviews*, v. 24, p. 325–342, 2013.

104 ABOELWAFA, O. et al. A review on solar Rankine cycles: Working fluids, applications, and cycle modifications. *Renewable and Sustainable Energy Reviews*, v. 82, p. 868–885, 2017.

105 PARK, B.-S. et al. Review of Organic Rankine Cycle experimental data trends. *Energy Conversion and Management*, v. 173, p. 679–691, 2018.

106 ASHRAE. *ASHRAE Addendum c for Standard 34-2019 (Novermber 19, 2019)*. Atlanta, GA, 2019.

107 ASHRAE. *ASHRAE Addendum f for Standard 34-2019 (Novermber 19, 2019)*. Atlanta, GA, 2019.

108 PRAXAIR. *Trans-2-Butene Safety Data Sheet P-4578*. [S.l.]: PRAXAIR, 2019. https://www.praxair.com/-/media/corporate/praxairus/documents/sds/trans-2-butene-c4h8-safety-data-sheet-sds-p4578.pdf?la=en&rev=745e815cac64449e9d37f3afd2d43a9b.

109 NHS-UK. *Acetone Safety Data Sheet*. [S.l.]: NHS, 2015. https://www.nhsggc.org.uk/media/236208/msds-acetone.pdf.

110 ROTH, C. *Isohexane Safety data sheet*. [S.l.]: CARL ROTH Gmbh & Co., 2019. https://www.carlroth.com/com/en/a-to-z/isohexane/p/2667.1.

111 GUO, C. et al. Performance analysis of compressed air energy storage systems considering dynamic characteristics of compressed air storage. *Energy*, Pergamon, v. 135, p. 876–888, sep 2017.

112 HE, W. et al. Exergy storage of compressed air in cavern and cavern volume estimation of the large-scale compressed air energy storage system. *Applied Energy*, v. 208, p. 745–757, 2017.

113 LUO, X. et al. Feasibility study of a simulation software tool development for dynamic modelling and transient control of adiabatic compressed air energy storage with its electrical power system applications. *Applied Energy*, v. 228, p. 1198–1219, 2018.

114 HE, W. et al. Study of cycle-to-cycle dynamic characteristics of adiabatic Compressed Air Energy Storage using packed bed Thermal Energy Storage. *Energy*, v. 141, p. 2120–2134, 2017.

115 SCIACOVELLI, A. et al. Dynamic simulation of Adiabatic Compressed Air Energy Storage (A-CAES) plant with integrated thermal storage – Link between components performance and plant performance. *Applied Energy*, v. 185, p. 16–28, 2017.

116 KRAWCZYK, P. et al. Comparative thermodynamic analysis of compressed air and liquid air energy storage systems. *Energy*, v. 142, n. 1, p. 46–54, 2017.

117 ZHANG, T. et al. Thermodynamic analysis of a novel hybrid liquid air energy storage system based on the utilization of LNG cold energy. *Energy*, v. 155, p. 641–650, 2018.

118 GEORGIOU, S.; SHAH, N.; MARKIDES, C. N. A thermo-economic analysis and comparison of pumped-thermal and liquid-air electricity storage systems. *Applied Energy*, v. 226, p. 1119–1133, 2018.

119 LOZOWSKI, D. *Chemical Engineering Plant Cost Index: 2018 Annual Value*. [S.l.]: Chemical Engineering, 2020. https://www.chemengonline.com/2019-cepci-updates-january-prelim-and-december-2018-final. Accessed: 2020-01-21.

120 GUIZZI, G. L. et al. Thermodynamic analysis of a liquid air energy storage system. *Energy*, v. 93, p. 1639–1647, 2015.

121 TAFONE, A. et al. New parametric performance maps for a novel sizing and selection methodology of a Liquid Air Energy Storage system. *Applied Energy*, v. 250, p. 1641–1656, 2019.